

University of Missouri-Rolla
Rolla, Missouri 65401

(NASA-CR-158094) TRANSPORT PROPERTIES IN
THE ATMOSPHERE OF JUPITER Progress Report,
Jan. 1977 - Dec. 1978 (Missouri Univ.
-Rolla.) 91 p HC A05/MF A01 CSCL 03B

N79-16785

Unclas
G3/91 43641

TRANSPORT PROPERTIES IN THE ATMOSPHERE OF JUPITER

Progress Report
January, 1977 - December, 1978
NASA Research Grant NSG 1369

Louis Biolsi Jr.
Chemistry Department



Table of Contents

	<u>Page</u>
I. Introduction	1
II. Transport Properties in the Pure Jovian Atmosphere	1
A. The Interaction Potentials	2
B. Errors in the Interaction Potentials	3
C. Errors in the Ion-Ion Interactions	4
III. Transport Properties of Monatomic Carbon	5
A. Ground State Interaction Potentials	6
1. Use of the Hulburt-Hirschfelder Potential	7
2. The Perfect Pairing Method	9
B. Excited State Interaction Potentials	11
IV. Transport Properties at the Mixing Boundaries	13
A. The Interaction Potentials	14
B. Errors in the Interaction Potentials	16
V. Some Atom-Molecule and Molecule-Molecule Interactions	16
A. The Interaction Potentials	17
B. Errors in the Interaction Potentials	23
VI. Other Collision Integrals	24
VII. Transport Properties of Air	25
References	26-28
Tables	29-86
Figure	87
Publications and Presentations	88

Tables of Transport Collision Integrals

<u>Interaction</u>	<u>Table</u>
H-H	3
He-He	4
H ₂ -H ₂	5
H ₂ -H	6
H ₂ -H _e	7
H-He	8
H-H ⁺	9
H-e	10
He-H ⁺	11
He-e	12
H ⁺ -H ⁺	13
He ⁺ -He ⁺	13
H ⁺ -He ⁺	13
e-e	14
H ⁺ -e	15
He ⁺ -e	15
H-He ⁺	16
He-He ⁺	17
C(³ P)-C(³ P)	21
C(³ P)-C(¹ D)	31
C(¹ D)-C(¹ D)	33
O-O	38
C-H	40
H-O	41
C-O	43
CO-CO	45
He-C ₂ H	47
C-C ₂	50
C ₂ -C ₂	52
He-O	55
He-C	56
C ⁺ -H	57
C-C ⁺	58

I. INTRODUCTION

The work discussed in this report is concerned with the calculation of transport properties near the surface of a probe entering the atmosphere of Jupiter. The discussion of this work is divided into the following categories; (1) transport properties in the pure Jovian atmosphere, (2) transport properties for collisions between monatomic carbon atoms, including the effect of excited electronic states, (3) transport properties at the boundaries for mixing of the pure Jovian atmosphere and the "atmosphere" due to the injection of gaseous ablation products, and (4) transport properties for interactions involving some of the molecular ablation products.

The transport properties are calculated using the kinetic theory of gases. This theory is well developed¹ for elastic collisions involving neutral atoms and/or small polyatomic (usually diatomic) species. The theory is in reasonably good shape for collisions involving ions.² The calculation of the contribution of inelastic collision effects to the transport properties is still quite difficult.³

The determination of the interaction potential between the interacting atoms/ions/molecules is usually the primary problem in the calculation of the transport properties. Transport collision integrals have been calculated for only a limited set of empirical and semiempirical interaction potentials.⁴ Since the accuracy of the fit of these empirical potentials to the "true" potential usually determines the accuracy of the calculation of the transport properties, a discussion of the various interaction potentials used in these calculations will be emphasized in this report.

II. TRANSPORT PROPERTIES IN THE PURE JOVIAN ATMOSPHERE

The nominal chemical composition of the Jovian atmosphere is taken to be $X_{H_2} = 0.89$ and $X_{He} = 0.11$, where X denotes mole fraction. If it is assumed that the atmosphere is at chemical equilibrium, the mole fractions of various species as

a function of temperature given in Table 1 are obtained.⁵ The table lists temperatures to 25,000°K since the calculations of Moss, et al.,^{6,7} indicate that high temperatures are attained near a probe upon entry into the Jovian atmosphere.

A. The Interaction Potentials

Transport properties for the species listed in Table 1 have been reported.⁸ The discussion given in that paper⁸ will not be repeated in this report. However, it is useful to review the interaction potentials used in the calculations since the potentials are the single most important "ingredient" in the calculation.

Many of the species in the Jovian atmosphere interact according to a potential which is repulsive at short range but possesses an attractive potential well at intermediate separations. Such interactions have been represented by one of the empirical (or semiempirical) potentials given below; (a) the attractive inverse power (AIP) potential,

$$V(r) = - \frac{A}{r^B} \quad (1)$$

where V is the potential energy, r is the internuclear separation, and A and B are adjustable parameters, (b) the exponential-six (ES) potential,

$$V(r) = \frac{\epsilon}{1 - \frac{6}{\alpha}} \left[\frac{6}{\alpha} e^{\alpha(1-r/r_e)} - \left(\frac{r_e}{r}\right)^6 \right] \quad (2)$$

where ϵ is the depth of the potential well, r_e is the value of r when $V = -\epsilon$, and α is an adjustable parameter, or (c) the Morse potential (MP),

$$V(r) = \epsilon \left[e^{-2 \frac{c}{\sigma}(r-r_e)} - 2e^{-\frac{c}{\sigma}(r-r_e)} \right] \quad (3)$$

where c is an adjustable constant and

$$\sigma = \frac{r_e}{1+0.693/c}$$

Other species in the Jovian atmosphere interact according to a potential which is repulsive at all separations. Such interactions have been represented by the exponential repulsive (ER) potential;

$$V(r) = Fe^{-Dr} \quad (4)$$

where D and F are adjustable constants.

Transport collision integrals have been calculated and tabulated for each of the potentials given above; AIP-reference 9, ES-reference 10, MP-reference 11, and ER-reference 12. Results for the interactions of interest in the Jovian atmosphere are summarized in Table 2. The third column lists the papers in which the "ab initio" calculations of the interactions listed in the first column are discussed and the fourth column lists the papers in which a "best fit" of the empirical potentials to the ab initio results is discussed.

In addition, the screened Coulomb potential is used for the ion-ion, ion-electron, and electron-electron interactions. For ions with unit electrical charge, the potential has the form²³

$$V(r) = \pm \frac{e^2}{r} e^{-r/\lambda_d} \quad (5)$$

where e is the electrical charge and λ_d is the Debye shielding distance, given by

$$\lambda_d = \left(\frac{kT}{4\pi e^2 n_e} \right)^{1/2}$$

and n_e is the electron density. The transport collision integrals have been tabulated for this potential.^{23,24}

Also, the $H-H^+$ and $He-He^+$ diffusion collision integrals were obtained by considering resonant charge exchange, the collision integrals for the $H-e$ interaction were obtained from data on low energy elastic scattering cross sections, and the $He-e$ collision integrals were obtained from data on the diffusion cross section.⁸

The resulting transport collision integrals for the interactions occurring in the pure Jovian atmosphere are shown in Tables 3 to 17. These collision integrals have been used to calculate the transport properties of each component and of the gas mixture.⁸

B. Errors in the Interaction Potentials

As indicated previously, the primary source of error is in the fitting of the empirical potentials for which the transport collision integrals are tabulated to the ab initio potentials, for which the collision integrals have not been calculated.

An example of the fit is shown in Table 18 for the He-H^+ interaction. The results in the second column are a representation of the accurate quantum mechanical calculations of Evett¹⁸ near r_e and the somewhat less accurate estimates of Mason and Vanderslice²² at large values of r . The results in the third column represent the "best fit" of the Morse potential to the ab initio results. Clearly the fit is relatively poor at small and large values of r but quite good near $r = r_e$. The reason for this is that the attractive region of the potential dominates the scattering process when¹

$$T^* = \frac{kT}{\epsilon} < \sim 5 \text{ or } 6$$

For the He-H^+ interaction, $T^* = 1.142$ when $T = 25,000^\circ\text{K}$. Thus the Morse parameters have been chosen so that the best fit to the ab initio results is at $r = r_e$.

The results in Table 18 are quite typical although, for some interactions, the curve fit is much poorer. Recent work concerned with improving the fit of the empirical potentials to the ab initio results will be discussed later.

C. Errors in the Ion-Ion Interactions

The second major source of error in determining the transport properties in the pure Jovian atmosphere is a consequence of the approximations used in the calculation of the ion-ion collision integrals. The Chapman-Enskog method was used to calculate these collision integrals, using the screened Coulomb potential and assuming static screening by electrons only. Also, only the lowest order approximation was used in calculating the collision integrals.

The lowest order approximation may be satisfactory for a highly ionized gas, in which case dynamic shielding results are very similar to the results obtained for static shielding by electrons only.²⁵ However, the third^{25,26} or higher²⁷ order terms in the Chapman-Enskog series should probably be included in the calculation in order to get good convergence to the "true" results for the transport properties. The convergence is particularly slow for transport properties that depend primarily on the electron distribution (such as the electron-electron and electron-ion binary diffusion coefficients, the thermal conductivity at high ionization, and the electrical conductivity) and is "rapid" for transport properties that depend primarily

on the heavy particle (atoms and ions) distributions (such as the viscosity, the thermal conductivity at low ionization, and the heavy particle binary diffusion coefficients).

At low ionization (less than $\sim 10\%$), the convergence problems are even greater.^{25,28} Under these conditions, the ionized gas approaches a Lorentzian mixture (i.e. a few light particles and many heavy, stationary particles). It has been shown^{25,29} that the calculation of the transport properties by considering a perturbation on the Lorentzian distribution is more efficient than the Chapman-Enskog approach (i.e. it converges rapidly).

The corrections at low and high ionization discussed above should be made for the ion and electron transport collision integrals. Also, the electric and magnetic fields in the Jovian atmosphere due to the presence of ions and electrons (and other causes) have an effect on the transport properties.

III. TRANSPORT PROPERTIES OF MONATOMIC CARBON

Entry probe heat shields are usually made of carbonaceous materials such as carbon-phenolic ablators: typically 92% carbon, 6% oxygen, and 2% hydrogen by mass.⁷ Ablative injection of the carbon-phenolic material into the shock layer is an important mechanism for reducing the intense radiative heating encountered during entry into the atmospheres of the outer planets. The species C, C₂, and C₃ are important ablative species, especially at low temperatures and near the entry probe. This is shown³⁰ in Table 19. Note that C₃ is the predominant species near the surface of the probe. Thus it is particularly important that accurate estimates of the transport collision integrals be obtained for interactions involving C₃.

Transport collision integrals have been calculated for the interaction of two ground state carbon atoms.³¹ These calculations will be described in some detail since the results will be used to obtain collision integrals for the C-C₂, C₂-C₂, C-C₃, C₂-C₃, and C₃-C₃ interactions. Thus it is important to obtain the best possible estimate of the C-C transport collision integrals (which means obtaining

the best possible estimate of the C-C interaction potentials).

A. Ground State Interaction Potentials

When two ground state (3P) carbon atoms interact, they can follow³² any of 18 interaction curves, corresponding to 18 molecular states of C_2 . Accurate interaction potentials are needed for each of these 18 states. Thirteen of the states possess an attractive potential well (bound states) and the spectroscopic constants (i.e. the dissociation energy, ϵ , the internuclear separation at the minimum in the potential well, r_e , the fundamental vibrational frequency, ω_e , the rotational constant, B_e , the anharmonicity constant, $\omega_e x_e$, and the rotation-vibration coupling constant, α_e) have been either measured experimentally³³ or accurately estimated.^{34,35} Five of the states are repulsive states.

These 18 states are listed in Table 20. The last five states are the repulsive states.

The interaction potentials for the 13 bound states can be represented by the Hulburt-Hirschfelder (HH) potential,^{36,37} given by

$$V(r) = \epsilon[(1-e^{-x})^2 + Cx^3e^{-2x}(1+bx)] \quad (6)$$

where

$$\begin{aligned} x &= \frac{\omega_e}{2r_e \sqrt{B_e \epsilon}} (r-r_e) & C &= 1 + a_1 \sqrt{\frac{\epsilon}{a_0}} \\ b &= 2 - \frac{7/12 - \epsilon a_2/a_0}{C} & a_0 &= \frac{\omega_e^2}{4B_e} \\ a_1 &= -1 - \frac{\alpha_e \omega_e}{6B_e^2} & a_2 &= \frac{5}{4} a_1^2 - \frac{2\omega_e x_e}{3B_e} \end{aligned}$$

This empirical potential uses the six spectroscopic constants as parameters and is nearly as accurate a representation of the "true" potential energy curve as is available^{36,38,39} (alternatives will be discussed later). It also has the intellectually satisfying feature that all parameters are fixed by experiment; i.e. it has no adjustable parameters.

The Hulburt-Hirschfelder potential energy curves were obtained for each of the first 13 states listed in Table 20. Unfortunately, until recently (recent developments will be discussed later), transport collision integrals had not been calculated for this potential. Thus the Hulburt-Hirschfelder curves were best fit with the Morse potential, as described previously. The best fit parameters are shown in the third column of Table 20.

Theoretical results³⁴ for three of the repulsive states were best fit with the exponential repulsive potential. The best fit parameters are also shown in the third column of Table 20. The $^3\Sigma_u^+$ and $^5\Sigma_g^+$ states were assumed to be degenerate with the $^3\Sigma_u^+$ and $^5\Sigma_g^+$ states, respectively, although, as will be discussed later, this assumption can be avoided.

Transport collision integrals for each of the Morse and exponential repulsive curves were calculated and then averaged according to their degeneracies.¹⁶ The results are shown in Table 21. These results were used³¹ to calculate the transport properties in a gas of 3P carbon atoms.

1. Use of the Hulburt-Hirschfelder Potential

It is important to emphasize again that an accurate $C(^3P)-C(^3P)$ interaction potential is highly desirable since this potential will be used as the basis for constructing interaction potentials for interactions involving C, C_2 , and C_3 .

The primary source of error for the $C(^3P)-C(^3P)$ interaction potentials is due to errors in the curve fit of the Morse potential to the accurate Hulburt-Hirschfelder potential. An example of the "goodness" of the curve fit is shown in Table 22, for the $^1\Sigma_g^+$ state. As before, the fit has been optimized near r_e but, at large and small values of r , the two potentials are quite different. This leads to errors in the calculation of the transport collision integrals.

Until recently, tabulations of collision integrals for the Hulburt-Hirschfelder potential were not available. However, a previously developed program⁴⁰ for calculating collision integrals has now been modified and adapted for the Hulburt-

Hirschfelder potential. Indeed, it will even calculate collision integrals for states with a "wobble" at large values of r such as the $1\pi_g$ state of C_2 shown in Table 23. Such wiggles may be real and not simply an artifact of the potential.³⁶ They seem to occur often for the states of C_2 .³⁴ One possible cause of the wiggles is rotational instability^{32,41} in C_2 .

Thus transport collision integrals can now be calculated for the Hulburt-Hirschfelder potential. Results for the states of C_2 are now being calculated. Results for the appropriate interactions in the pure Jovian atmosphere will also be calculated.

Some results are available. Table 24 lists the transport collision integrals for the $1\Sigma_g^+$ state of C_2 for the Hulburt-Hirschfelder and the Morse potentials. The differences are quite substantial. These differences are directly reflected in the calculation of the transport properties of 3P carbon atoms. They will also be reflected (although not directly) in the calculation of transport properties in a gas mixture containing 3P carbon atoms.

The value of σ for the Hulburt-Hirschfelder potential was taken to be the value of r (other than $r = \infty$) for which $V(r) = 0$. It was calculated by an iterative method, using the relation

$$2e^{A(t-1)} = B(t-1)^3[1 + G(t-1)] + 1$$

where

$$t = \frac{\sigma}{r_e} \quad A = \frac{\omega_e}{2\sqrt{B_e}\epsilon} \quad B = CA^3 \quad G = bA$$

For the Hulburt-Hirschfelder potential, $\sigma = 0.9494\text{\AA}$ while $\sigma = 0.9724\text{\AA}$ for the Morse potential. Thus most of the difference in the results for the two potentials is in the calculation of $\Omega^{(1,1)*}$ and $\Omega^{(2,2)*}$.

How accurate is the Hulburt-Hirschfelder potential? While other potentials, with adjustable parameters, may give a better fit to the "true" potential for specific chemical species, probably no other empirical or semiempirical potential gives a better fit to true potentials for a wider range of chemical species.³⁸

It should be pointed out that, while the Hulburt-Hirschfelder potential is based on experimental information, it is also model dependent since the spectroscopic constants are calculated by assuming that molecules are anharmonic vibrators and non-rigid rotors. However, a method is available for determining potential energy curves which makes use of the experimental energy levels directly (i.e. it is not model dependent) and also does not depend on assuming a functional form for the potential; i.e. the results are obtained in the form of a table of $V(r)$ versus r . This method was developed by Rydberg,⁴² Klein,⁴³ and Rees⁴⁴ and is called the RKR method. It gives results that agree with the results obtained by the Dunham method⁴⁵ near r_e .^{46,47} The RKR method is the most accurate method for determining the interaction potential energy between atoms that interact according to a long range attractive potential.

Table 25 gives a comparison of the RKR results⁴⁸ with the Hulburt-Hirschfelder results for the $1\Sigma_g^+$, $3\Pi_u$, and $1\Pi_g$ states of C_2 . The agreement tends to be very good near r_e but differences can be substantial at large values of r . These results, and others, indicate that the Hulburt-Hirschfelder potential is quite accurate, especially near r_e , the region that usually makes the predominant contribution to the scattering.

It should be pointed out that the computer program that has been developed can take $V(r)$ versus r "data", fit it with a polynomial, and calculate the transport collision integrals for the resulting polynomial curve fit; i.e. an assumed functional form for the potential is not required. Thus transport collision integrals can be obtained directly from the RKR results, if necessary.

2. The Perfect Pairing Method

It was previously assumed³¹ that the $3\Sigma_{u2}^+$ and $5\Sigma_{g2}^+$ states are degenerate with the $3\Sigma_u^+$ and $5\Sigma_g^+$ states, respectively, since good quantum mechanical calculations of the interaction energy are not available for these states. However, an approximate method of estimating the potential energy for these states based on valence bond theory,⁴⁹ called the perfect pairing method, is available. This method will be described briefly.

If it is assumed that eight electrons in C_2 fill the four lowest molecular orbitals, i.e.

$$(\sigma_g 1s)^2 (\sigma_u^* 1s)^2 (\sigma_g 2s)^2 (\sigma_u^* 2s)^2$$

then, among the possible arrangements for the four remaining electrons, are the arrangements corresponding to the $^3\Sigma_{u2}^+$ and $^5\Sigma_{g2}^+$ states^{50,51} shown in Table 26, along with arrangements for the $^3\Pi_u$ and $^3\Sigma_g^-$ states. The direction of each arrow corresponds to the "direction of the spin".

The energy relationships are simple. They are based on a valence bond treatment that is correct at large values of r . The Coulomb integral is assumed to make no contribution to the energy and there is a contribution to the energy of $\frac{1}{2} J$ (J is the exchange integral) from each electron in a bonding molecular orbital and contribution of $-\frac{3}{2} J$ from each electron in an antibonding orbital.⁵¹ Also

$$J_{xx} = J_{yy}$$

Thus

$$V(^3\Sigma_{u2}^+) = -J_{zz} + J_{xx} \quad V(^5\Sigma_{g2}^+) = -2J_{xx}$$

The integrals J_{xx} and J_{zz} must be evaluated using information about two states for which potential energy curves are known. The $^3\Pi_u$ and $^3\Sigma_g^-$ states have been used for this purpose since accurate RKR results are available for these states⁴⁸ and the RKR results are accurately reproduced by the Hulburt-Hirschfelder potential. For these states

$$V(^3\Pi_u) = \frac{1}{2} J_{zz} + \frac{3}{2} J_{xx} \quad V(^3\Sigma_g^-) = J_{zz} + J_{xx}$$

or

$$J_{xx} = \frac{2V(^3\Pi_u) - V(^3\Sigma_g^-)}{2} \quad J_{zz} = \frac{3}{2} V(^3\Sigma_g^-) - V(^3\Pi_u)$$

Using the known values of $V(^3\Pi_u)$ and $V(^3\Sigma_g^-)$, the quantities J_{xx} and J_{zz} , and thus $V(^3\Sigma_{u2}^+)$ and $V(^5\Sigma_{g2}^+)$, can be estimated. The results are shown in Table 27. These results can be curve fit with one of the empirical repulsive potentials and the transport collision integrals can then be determined.

When the calculations discussed in sections III-A-1 and III-A-2 are completed, a substantially improved estimate of the transport properties of ground state carbon atoms will be available.

B. Excited State Interaction Potentials

The temperatures attained during entry of a probe into the Jovian atmosphere are so high that a significant fraction of the carbon atoms are in excited electronic states. This is shown in Table 28, obtained by including all of the electronic states listed in the JANAF Tables³⁵ in the calculation and assuming that there is an equilibrium distribution of atoms among the states. Clearly, at temperatures above 6000°K, excited electronic states are significantly populated.

In previous reports,^{52,53} possible models for calculating the contribution to the transport properties from species in excited electronic states were discussed. Since the results obtained using these models are less reliable than the results to be presented below, these models will not be discussed in this report. However, the model calculations do confirm the assumption⁵⁴ that the contribution from low lying excited electronic states to the transport properties is nearly the same as the contribution from the ground state and that the contribution from highly excited electronic states to the transport properties is negligible.

Now consider the interaction between a ground state (3P) carbon atom and a carbon atom in the first excited (1D) electronic state. The molecular states of C_2 that dissociate into a 3P carbon atom and a 1D carbon atom are shown^{32,34} in the first column of Table 29. Experimental values of the spectroscopic constants are available³² for the $^3\Pi_{g3}$ state. For the other bound states (except the $^3\Pi_{u2}$ state), theoretical results^{34,35} have been correlated in order to obtain reasonable estimates of the spectroscopic constants.³⁵ The results are shown in Table 29. The $^3\Phi_u$, $3\Delta_g$, $^3\Sigma_g^+$, and $^3\Sigma_u^-$ repulsive states were investigated theoretically by Fougere and Nesbet.³⁴ However, the level of refinement of their calculations for these states is relatively crude.

For the ${}^3\Pi_{g2}$ and ${}^3\Pi_{u2}$ bound states, Morse parameters were obtained by making a best fit of the Morse potential to the theoretical results of Fougere and Nesbet.³⁴ For the other bound states, the Morse parameters were obtained by making a best fit of the Morse potential to the Hulburt-Hirschfelder potential.

In principle, collision integrals for the repulsive states should be obtained by using an empirical repulsive potential. However, while at the level of calculation III by Fougere and Nesbet,³⁴ the ${}^3\Phi_u$, ${}^3\Delta_g$, and ${}^3\Sigma_u^-$ states are repulsive, at the level of their least accurate calculation (called calculation I--the only level at which results are available for these states), these three states exhibit a shallow attractive minimum in the potential. Thus Fougere and Nesbet's results for these states³⁴ have been best fit with the Morse potential, using the "spectroscopic constants" listed in Table 30. Clearly this is a rather crude approach.

The parameters obtained for the empirical potentials are given in Table 30. Notice that the last eight states listed in Table 30 have not been included in the calculation. This is a serious source of error. However, a crude estimate of the potential energy curve for each of these states can be obtained by using the perfect pairing method, discussed previously.

Transport collision integrals can be obtained for each of the first ten states listed in Table 30 and the integrals can then be averaged according to their degeneracies.¹⁶ The results are given in Table 31. In addition to the errors due to ignoring the contribution to the collision integrals from eight states, the other sources of error discussed in connection with the $C({}^3P)$ - $C({}^3P)$ calculation are sources of error for this calculation.

Now consider the interaction between two 1D carbon atoms. The molecular states of C_2 that dissociate into two 1D carbon atoms are shown³⁴ in the first column of Table 32. Experimental spectroscopic constants are not available for any of these states. The estimated spectroscopic constants³⁴ for the bound states are also shown in Table 32. At the level of calculation III by Fougere and Nesbet,³⁴ the ${}^1\Pi_g$ and

$^1\phi_u$ states are repulsive, but they exhibit a shallow attractive minimum at the level of calculation I.

The first seven states listed in Table 32 have been best fit with the Morse potential. The resulting parameters are given in Table 32. The last eight states listed in Table 32 have been ignored in the calculation. This is, of course, a serious source of error but the perfect pairing method can be used to obtain estimates of the potential energy curves for these repulsive states.

Transport collision integrals for the first seven states listed in Table 32 have been obtained and averaged according to their degeneracies.¹⁶ The results are given in Table 33. The sources of error discussed previously also apply to these results.

It is clear that experimental and/or theoretical information for the excited electronic states of carbon is rather limited. Thus the results in Tables 31 and 33 must be considered to be relatively crude first order estimates. However, the results are almost certainly accurate to within less than a factor of 2 and the inclusion of perfect pairing results for the omitted states will probably not change the transport collision integrals significantly.

The results in Table 33 can be used to calculate¹ the transport properties in a gas of 1D carbon atoms. It is of greater interest, however, to use the results in Tables 21, 31 and 33 to calculate^{1,8} the transport properties in a mixture of 3P and 1D carbon atoms. Some results for the translational contribution to the thermal conductivity, λ_{tr}^{mix} , are given in Table 34. Notice that the results when $X_{3p} \neq 1.00$ are not very different from the results when $X_{3p} = 1.00$ which is, again, consistent with the assumption⁵⁴ that the contribution to the transport properties from low lying excited electronic states is similar to the contribution from the ground state.

IV. TRANSPORT PROPERTIES AT THE MIXING BOUNDARIES

During entry of a probe into the Jovian atmosphere, mixing of the ablative species with the pure atmosphere begins³⁰ at 12% of the distance from the probe to

the shock front (0.294 cm from the probe) for stagnation-point peak heating. The temperature at this inner mixing boundary is 7775°K. The mole fractions of the various species at this boundary are shown in the second column of Table 35.

Mixing of the ablative species with the pure atmosphere terminates³⁰ at 22% of the distance from the probe to the shock front (0.539 cm from the probe). The temperature at this outer mixing boundary is 14,756°K. The mole fractions of the various species at this boundary are shown in the third column of Table 35. The constant pressure across the shock layer is 6.29 atmospheres.

Assume that, at the inner mixing boundary, the only species that need to be considered are C, H, and O ($X_{\text{total}}=0.953$). The possible two body interactions are shown in Table 36. The O-O, C-H, C-O, and H-O interactions have not yet been considered. Also assume that, at the outer mixing boundary, the only species that need to be considered are H, e, H^+ , and He ($X_{\text{total}}=0.999$). The possible two body interactions are shown in Table 36. All of these interactions have been considered previously.

A. The Interaction Potentials

The calculation of the transport properties at these boundaries has been considered in some detail^{56,57} and the discussion will not be repeated in this report. However, the calculation of the O-O, C-H, C-O, and H-O interaction potentials will be reviewed.

Transport collision integrals for the O-O interaction were obtained to 15,000°K by Yen and Mason.⁵⁸ The possible molecular states of O_2 that dissociate into two ground state (3P) oxygen atoms are the same as the molecular states of C_2 that dissociate into two ground state carbon atoms, given in Table 20. For some of the O_2 bound states, RKR and/or Hulburt-Hirschfelder results^{51,59} were best fit⁵⁸ with empirical potentials for which the transport collision integrals are tabulated. For other bound states and the repulsive states, the perfect pairing method was used⁵¹ to obtain the interaction potentials which were then best fit⁵⁸ with empirical potentials. The empirical potential parameters⁵⁸ are shown in Table 37.

The transport collision integrals obtained by Yun and Mason⁵⁸ are given in Table 38. Values above 15,000°K have been extrapolated from a plot of \ln (collision integral) versus \ln (T).

Now consider the C-H interaction. The states of CH that dissociate into ground state carbon and hydrogen atoms are³² listed in Table 39. Spectroscopic information is available^{32,35} for the $^2\Pi$ and $^2\Sigma$ bound states and theoretical information is available for the $^4\Sigma$ bound state⁶⁰ and for the repulsive $^4\Pi$ state.⁶¹

The Morse potential was best fit to the Hulburt-Hirschfelder curve for the $^2\Pi$ state and to the theoretical calculations⁶⁰ for the $^4\Sigma$ and $^2\Sigma$ states. The exponential repulsive potential was best fit to the theoretical calculations⁶¹ for the $^4\Pi$ state. The resulting parameters are shown in Table 39. Transport collision integrals were obtained for each state and then averaged according to their degeneracies.¹⁶ The results are given in Table 40.

Now consider the H-O interaction. The states of OH that dissociate into ground state oxygen and hydrogen atoms are³² listed in Table 39. Spectroscopic constants are available^{32,35} for the $^2\Pi$ and $^2\Sigma$ bound states but neither experimental nor theoretical information is available for the $^4\Pi$ and $^4\Sigma$ repulsive states. Thus they have been ignored in the calculation, a serious source of error. However, potential energy curves for these states can be estimated by using the perfect pairing method.

The Morse potential was best fit to the Hulburt-Hirschfelder results for the $^2\Pi$ and $^2\Sigma$ states. The resulting parameters are shown in Table 39. Transport collision integrals were obtained for each state and then averaged according to their degeneracies.¹⁶ The results are given in Table 41.

Now consider the C-O interaction. The states of CO that dissociate into ground state carbon and oxygen atoms are³² listed in Table 42. The spectroscopic constants are known^{32,35} for the lowest lying bound state, the $^1\Sigma^+$ state. The next lowest lying bound state of CO, the $^3\Pi_r$ state, does not dissociate into ground state atoms.⁶² Thus the other states listed in Table 42 have been ignored in the calculation.

The Morse potential was best fit to the Hulburt-Hirschfelder results for the $1\Sigma^+$ state and the transport collision integrals were calculated. The results are given in Table 43.

Using the results discussed above, the transport properties at the mixing boundaries can be calculated.^{56,57}

B. Errors in the Interaction Potentials

A major improvement in the results would be obtained by calculating the transport properties for the Hulburt-Hirschfelder potential, using the recently developed program, for those interactions for which the necessary spectroscopic constants are available.

The major source of error in the O-O calculations is due to the use of the relatively crude perfect pairing method to obtain interaction potentials for more than half the states. However, these results can probably be improved since Schaefer and Harris⁶³ have performed ab initio quantum mechanical calculations for 62 low lying states of O_2 . Their results for the repulsive states in Table 37 can be curve fit with empirical potentials. The results should be considerably more reliable than the results obtained using the perfect pairing method.

Half the states have been ignored in the H-O calculation, clearly a major source of error. Crude estimates of the potential energy curves for the omitted states can be obtained by using the perfect pairing method. It is also desirable to have an accurate estimate of the transport collision integrals for the H-O interaction since OH plays an important role in atmospheric photochemistry and photochemical smog.⁶⁴

All of the states of CO listed in Table 42, as well as the $3\Pi_r$ state, which dissociates into excited atoms, should be included in the C-O calculation. Spectroscopic information is available³² for the 1Π , $1\Sigma_2^+$, and $3\Pi_r$ states. Potential energy curves for the other states can be estimated using the perfect pairing method.

V. SOME ATOM-MOLECULE AND MOLECULE-MOLECULE INTERACTIONS

Transport properties near the surface of the probe will be determined primarily by the species near the surface. The mole fractions of the species at the surface

of the probe, where the temperature is 4268°K, are given³⁰ in Table 44. The species are all ablation products and most of them are diatomic or polyatomic species. Thus atom-molecule and molecule-molecule interactions must be considered as well as atom-atom interactions, the only type of interaction considered previously.

A. The Interaction Potentials

The determination of interaction potentials for atom-molecule interactions is usually difficult and the available methods are relatively crude. The problems are even greater for molecule-molecule interactions.

However, the CO-CO interaction has been considered in some detail. Mason and Rice⁶⁵ assumed that the interaction can be described by the exponential-six potential, using the parameters

$$\alpha = 17.0 \quad r_e = 3.937\text{\AA} \quad \epsilon/k = 119.1^\circ\text{K}$$

The resulting transport collision integrals are given in Table 45. Since Mason and Rice⁶⁵ determined the parameters by comparison with experimental data on viscosities, the results in Table 45 should be quite accurate.

The CO-CO interaction is one of the few interactions involving molecules for which such a relatively straightforward procedure is available. The He-C₂H interaction will be used to illustrate a method (called the peripheral force method) for calculating interaction potential energies for interactions involving molecules. This method incorporates the assumptions that the centers of force in a molecule are located at the nucleus of each atom and that all atoms can be treated as independent entities.⁶⁶ The name "peripheral" derives from the assumption that atoms "hidden" in the interior of molecules are not involved in the intermolecular interactions; i.e. for the He-CH₄ interaction, reasonable agreement with experiment is obtained by assuming that there is no He-C interaction.⁶⁷ The peripheral force model has been developed primarily for inverse power repulsive potentials.

The He-C₂H interaction will be used to illustrate the method since it can be assumed that the two body interactions are inverse power repulsive for this system and this system illustrates how the method can be applied to heteronuclear linear

triatomic molecules, since C_2H is linear^{68,69} with the geometry $C^1-C^2-H^3$ where the superscripts 1, 2, and 3 label the atoms. Two "extremes" are possible during He- C_2H collisions; (1) it can be assumed that there are twice as many C-He collisions as H-He collisions which probably overcounts C-He collisions, and (2) it can be assumed that He rarely collides with the "center" carbon atom, C^2 (an assumption consistent with the peripheral atom assumption); i.e. the number of C-He and H-He collisions are the same. Case 2 probably undercounts C-He collisions but, perhaps, not by much since it has been shown⁷⁰ that, for Ar- CO_2 collisions (CO_2 has the linear geometry O-C-O), the Ar-C collisions are negligible. Only the first extreme case will be considered since the potentials used are quite crude and this case better illustrates the application of the peripheral force method to triatomic molecules.

The coordinate system used for the He- C_2H interaction is given in Figure 1. The symbol r denotes the distance from the helium atom to the center of geometry of the C_2H specie. The symbols R_1 , R_2 , and R_3 denote the distances from the helium atom to each of the three atoms in the C_2H specie. The distances a_1 , a_2 , and a_3 are obtained from the estimated bond lengths;³⁵

C-C	1.207 $\overset{\circ}{\text{\AA}}$
C-H	1.061 $\overset{\circ}{\text{\AA}}$

The assumption of independent atoms implies the assumption that the potentials are additive⁶⁶ (which is certainly not true⁷¹); i.e.

$$V(\text{He-}C_2H) = V(\text{He-C}^1) + V(\text{He-C}^2) + V(\text{He-H}^3) \quad (7)$$

However, since the C_2H specie is "tumbling", it is necessary to average the atom-atom potentials (and thus the atom-molecule potential) over all angles. The averaging procedure takes the form⁶⁶

$$V(\text{atom-atom})_{av} = \frac{1}{4\pi} \int_0^\pi V(R) 2\pi \sin\theta d\theta \quad (8)$$

For repulsive inverse power (RIP) potentials with the form

$$V(R) = \frac{K}{R^s} \quad (9)$$

equation (8) becomes⁶⁶

$$V(\text{atom-atom})_{\text{av}} = \frac{1}{2} \int_0^\pi \frac{K}{R^s} \sin\theta d\theta \quad (10)$$

$$= V(r)\lambda(\alpha, s)$$

where use has been made of the law of cosines; i.e.

$$R = r(1 + \alpha^2 - 2\alpha\cos\theta)^{1/2}$$

and

$$V(r) = \frac{K}{r^s} \quad (11)$$

Also

$$\lambda(\alpha, s) = \frac{(1+\alpha)^{s-2} - (1-\alpha)^{s-2}}{2\alpha(s-2)(1-\alpha^2)^{s-2}} \quad (12)$$

and

$$\alpha = \frac{a}{r}$$

The values of a are given in Figure 1. Using equations (7) and (10), the angle averaged atom-molecule interaction is

$$V(\text{He-C}_2\text{H})_{\text{av}} = V(r)_{\text{He-C}1}\lambda(\alpha_1, s_1) + V(r)_{\text{He-C}2}\lambda(\alpha_2, s_2) + V(r)_{\text{He-H}3}\lambda(\alpha_3, s_3) \quad (13)$$

The atom-atom interactions are needed. Now⁷¹

$$V(\text{He-H}) = \frac{2.60}{R^{6.06}} \quad (\text{e.v.}) \quad (14)$$

The He-C interaction has not been studied from the point of view of this model.

However, since it is possible to approximate the Ar-C potential by using the Ar-N potential,⁷⁰ it is not unreasonable to approximate the He-C interaction by using the He-N potential, i.e.⁶⁶

$$V(\text{He-N}) \cong V(\text{He-C}) = \frac{13.7313}{R^{6.23}} \quad (\text{e.v.}) \quad (15)$$

However, this approximation is very crude since the justification⁷⁰ for the Ar-C potential is based on isoelectronic structures which is not applicable in this case.

Using the potentials given by equations (14) and (15) and the results in

Figure 1, the parameters to be used in the calculations are

$$\alpha_1 = \alpha_3 = \frac{1.134}{r} \quad \alpha_2 = \frac{0.073}{r}$$

$$s_1 = s_2 = 6.23 \quad s_3 = 6.06$$

Results for the four terms in equation (13) can now be calculated. The results for the averaged atom-atom interactions are shown in the second, third, and fourth columns

of Table 46. Notice that $V(\text{He-C}^2)$ is small (of the order of 10% or less) compared with $V(\text{He-C}^1)$ which is consistent with the assumption that the He-C^2 interaction can be ignored.

This result suggests that it should not be assumed that He-C^1 and He-C^2 interactions are equally probable. As a crude approximation, assume that the He-C^2 interactions are half as frequent as the He-C^1 interactions (an approximation "midway" between extreme cases 1 and 2). Thus equation (13) should be modified; i.e.,

$$V(\text{He-C}_2\text{H})_{\text{av}} = V(r)_{\text{He-C}^1} \lambda(\alpha_1, s_1) + \frac{1}{2} V(r)_{\text{He-C}^2} \lambda(\alpha_2, s_2) + V(r)_{\text{He-H}^3} \lambda(\alpha_3, s_3) \quad (16)$$

The resulting values of the averaged atom-molecule potential are given in the fifth column of Table 46.

The results for $V(\text{He-C}_2\text{H})_{\text{av}}$ have been best fit with the exponential repulsive potential in order to calculate the transport collision integrals. The best fit parameters are

$$F = 56117 \text{ e.v.} \quad D = 5.2002 \text{ cm}^{-1}$$

The resulting potential energy is shown in the sixth column of Table 46. Agreement with the results for $V(\text{He-C}_2\text{H})_{\text{av}}$ is reasonably good.

The transport collision integrals for the $\text{He-C}_2\text{H}$ interaction are shown in Table 47. These results have been used to calculate the binary diffusion coefficient.^{1,8} The results are shown in the second column of Table 48. Results obtained by Esch, et al.,⁷² using a much simpler model, are also shown in Table 48.

Now consider the C-C_2 interaction. It will no longer suffice to assume that all atom-atom interactions can be approximated by the repulsive inverse power potential. Results for $V(\text{atom-atom})_{\text{av}}$ should be obtained for each of the states of C_2 listed in Table 20, using the empirical potentials and parameters given in the table. Then, using the peripheral force model, $V(\text{C-C}_2)_{\text{av}}$ should be determined for each state from⁶⁶

$$V(\text{C-C}_2)_{\text{av}} = 2V(\text{C-C})_{\text{av}} \quad (17)$$

The results obtained for each state, using equation (17), should then be best fit with an empirical potential for which transport collision integrals have been

tabulated and the collision integrals should be averaged according to their degeneracies.¹⁶

Results have been obtained for the $1\Sigma_g^+$ ground state of C_2 . The "true" potential for this state has been best fit with the Morse potential. When the Morse potential is substituted into equation (8), the result is

$$V(C-C_2)_{av}(MP) =$$

$$\frac{\sigma\epsilon}{c\alpha r} e^{\frac{c}{\sigma} r} e^{-\frac{c}{\sigma} r} \{e^{-2mr(1+\alpha)} - e^{-2nr(1-\alpha)}\} - \frac{\sigma}{4cr} e^{\frac{c}{\sigma} r} e^{-2mr} - e^{-2nr}$$

$$+ 2\{e^{-mr(1+\alpha)} - e^{-nr(1-\alpha)}\} - \frac{2\sigma}{cr} \{e^{-mr} - e^{-nr}\} \quad (18)$$

where

$$m = \frac{c}{\sigma} (1+\alpha) \quad n = \frac{c}{\sigma} (1-\alpha)$$

Using equations (17) and (18) and the parameters given in Table 20 for the $1\Sigma_g^+$ state, the results shown in the second column of Table 49 are obtained. Notice that $V(r)$ becomes large and negative at small values of r . This must be an artifact of the integration and cannot be physical. The results for $V(C-C_2)_{av}$ have been best fit with the Morse potential. The best fit parameters (for $r \geq 0.6000\text{\AA}$) are

$$\epsilon = 6.93 \text{ e.v.} \quad r_e = 1.560\text{\AA} \quad c = 2.1677$$

The resulting potential energy is shown in the third column of Table 49. The fit to the results in the second column is not very good except near r_e where, as before, the curve fit was optimized. The transport collision integrals are given in Table 50.

Now consider the C_2-C_2 interaction, a molecule-molecule interaction. According to the peripheral force model, the orientation averaged potential energy for the C_2-C_2 interaction is⁶⁶

$$V(\text{molecule-molecule})_{av} = \frac{4}{(4\pi)^2} \int_0^\pi \int_{1-\alpha}^{1+\alpha} V(R) 2\pi \sin\theta_2 d\theta_2 2\pi \sin\theta_1 d\theta_1 \quad (19)$$

If the morse potential is used for $V(R)$, the result is

$$V(C_2-C_2)_{av}(MP) =$$

$$\frac{\epsilon\sigma^3}{4\alpha^2(cr)^3} e^{\frac{2c}{\sigma}(r-r_e)} \left[e^{-\frac{4c}{\sigma}\alpha r} (Mr+1) + e^{\frac{4c}{\sigma}\alpha r} (Nr+1) - 2 \frac{c}{\sigma} r - 2 \right]$$

$$+ \frac{2\epsilon\sigma^3}{4\alpha^2(cr)^3} e^{\frac{c}{\sigma}(r-r_e)} \left[4 + 2 \frac{c}{\sigma} r - e^{-\frac{2c}{\sigma}\alpha r} (Mr+2) - e^{-\frac{2c}{\sigma}\alpha r} (Nr+2) \right]$$

where

$$M = \frac{c}{\sigma} (1+2\alpha) \quad N = \frac{c}{\sigma} (1-2\alpha)$$

Again, only the $^1\Sigma_g^+$ ground state of C_2 has been considered. Using the parameters given in Table 20, the results given in the second column of Table 51 are obtained. As was the case for the C- C_2 interaction, the large negative values of $V(r)$ at small values of r must be an artifact of the integration and will be ignored. The results in the second column of Table 51 were best fit with the Morse potential. The best fit parameters (for $r \geq 1.058\text{\AA}$) are

$$\epsilon = 7.92 \text{ e.v.} \quad r_e = 1.867\text{\AA} \quad c = 3.4329$$

The resulting potential energy is shown in the third column of Table 51. The fit to the results in the second column is not very good except near r_e where, as before, the curve fit has been optimized. The transport collision integrals for the C_2-C_2 interaction are given in Table 52.

It is interesting to notice that the C-C, C- C_2 , and C_2-C_2 interactions become progressively "longer range"; i.e. the range of separations at which attractive interactions occur becomes progressively larger. This is shown explicitly in Table 53.

In addition

$$\epsilon_{C_2-C_2} > \epsilon_{C-C_2} > \epsilon_{C-C}$$

i.e. the "quasi-molecules" C_4 , C_3 , and C_2 have the following order of stability (according to these first order calculations);

$$C_4 > C_3 > C_2$$

The reason for these results is not entirely clear but one possible explanation is the relative polarizabilities of C and C_2 . The specie C_2 is almost certainly more

polarizable⁴ than C. Thus the long range attractive induced dipole-induced dipole forces would have the relative strengths

$$C_2-C_2 > C-C_2 > C-C$$

This order is consistent with the calculated results.

The results in Tables 21, 50, and 52 can be used to estimate the transport properties in a mixture^{1,8} of C and C₂. Some results for λ_{tr}^{mix} are given in Table 54.

8. Errors in the Interaction Potentials

The interaction potentials for the He-C₂H interaction are quite crude and this interaction was considered primarily to illustrate the application of the peripheral force model to interactions involving linear triatomic molecules. There are two main sources of error in this calculation. First, as already mentioned, the He-C interaction is almost certainly seriously in error.

Second, there does not appear to be any a priori method for assigning probabilities to the He-C¹ and He-C² collisions. The assumption that He-C² collisions are half as frequent as He-C¹ collisions seems intuitively reasonable on the basis of geometric and steric considerations but it is, of course, just a "good" guess.

The surprisingly good agreement between these results and those of Esch, et al.,⁷² shown in Table 48, is no reason for increased confidence in the results since the results of Esch, et al.⁷² are probably no more reliable than these results. They⁷² used the Lennard-Jones (6,12) potential; i.e.

$$V(r) = 4\epsilon \left[\left(\frac{\sigma}{r} \right)^{12} - \left(\frac{\sigma}{r} \right)^6 \right]$$

and estimated σ from a plot of σ versus molecular weight for known species and estimated ϵ from a plot of ϵ versus molecular weight for known species. The good agreement in Table 48 is intriguing but almost certainly fortuitous.

For the C-C₂ and C₂-C₂ interactions, only the $^1\Sigma_g^+$ ground state of C₂ has been included in the calculation. The 17 other states listed in Table 20 should also be included in the calculation. These calculations are in progress.

The Morse potential has been assumed to be the "true" potential for the C-C₂ and C₂-C₂ interactions. However, as discussed previously, the Hulburt-Hirschfelder potential is much more accurate. If the Hulburt-Hirschfelder potential is used for V(R) in equation (8), the result is

$$V(C-C_2)_{av(HH)} =$$

$$\begin{aligned} & \frac{\epsilon}{\alpha(xr)^2} e^{xr} [e^{-Pr}(Pr+1) - e^{-Qr}(Qr+1)] + \\ & \frac{\epsilon}{\alpha} cx^2 e^{2xr} [\{ (1+\alpha)^5 e^{-2Pr} - (1-\alpha)^5 e^{-2Qr} \} (-\frac{1}{2} b x r^3) \\ & + \{ (1+\alpha)^4 e^{-2Pr} - (1-\alpha)^4 e^{-2Qr} \} r^2 (-\frac{1}{2} - \frac{5}{4} b + 2bxr_e) \\ & + \{ (1+\alpha)^3 e^{-2Pr} - (1-\alpha)^3 e^{-2Qr} \} r (-\frac{1}{x} + \frac{3}{2} r_e + 4br_e - \frac{5}{2} \frac{b}{x} - 3bxr_e^2) \\ & + \{ (1+\alpha)^2 e^{-2Pr} - (1-\alpha)^2 e^{-2Qr} \} (-\frac{3}{2} \frac{1}{x^2} + \frac{9}{4} \frac{r_e}{x} - \frac{3}{2} r_e^2 + 6 \frac{br_e}{x} - \frac{9}{2} br_e^2 + 2bxr_e^3 - \frac{15}{4} \frac{b}{x^2}) \\ & + \{ e^{-2Pr}(2Pr+1) - e^{-2Qr}(2Qr+1) \} (-\frac{1}{4} \frac{1}{cx^4 r^2} - \frac{15}{8} \frac{b}{x^4 r^2} + 3 \frac{br_e}{x^3 r^2} - \frac{9}{4} \frac{br_e^2}{(xr)^2} + \frac{br_e^3}{xr^2}) \\ & - \frac{3}{4} \frac{1}{x^4 r^2} + \frac{9}{8} \frac{r_e}{x^3 r^2} - \frac{3}{4} \frac{r_e^2}{x^2 r^2} + \frac{1}{4} \frac{r_e^3}{xr^2} - \frac{1}{4} \frac{br_e^4}{r^2})] \end{aligned}$$

where

$$P = x(1+\alpha) \quad Q = x(1-\alpha) \quad x = \frac{(u)e}{2r_e \sqrt{B_e C}}$$

Calculations of the C-C₂ transport properties, using equation (21), are now in progress.

A general precaution about the use of the peripheral force model is necessary. Previous calculations using this model have been for interactions for which experimental data that can be used to check the potentials is available. The model seems to work reasonably well but it is not highly accurate.⁷⁰ Alternative models may be more accurate.^{70,73} It cannot necessarily be assumed that this model can be used for all systems of interest and it has been assumed as "an article of faith" that the peripheral force model can be applied to the C-C₂ and C₂-C₂ interactions.

VI. OTHER COLLISION INTEGRALS

Some other transport collision integrals which may be useful are given in Tables 55 to 58. The He-C results have been obtained by using the potential given

by equation (15). Thus, as discussed previously, the results are probably not very accurate. Results have not been given for $\sigma_{\Omega}^{2(1,1)*}$ for the C-C⁺ interaction since this collision integral should be determined from charge transfer.

VII. TRANSPORT PROPERTIES OF AIR

Using the recently developed program for calculating transport collision integrals for the Hulburt-Hirschfelder potential, as well as RKR results⁷⁵ for some of the bound states of O₂, significant improvements on the previously calculated⁵⁸ transport collision integrals of O₂ are possible. In addition, the Hulburt-Hirschfelder program, RKR results³⁸ for N₂, theoretical calculations,⁷⁶ and the perfect pairing method can be used to improve on the previously calculated⁵⁸ transport collision integrals of N₂. Using similar information and the peripheral force model, improved estimates of the N₂-N₂, O₂-O₂, and N₂-O₂ interactions can also be obtained. Thus the transport properties of air can be re-evaluated.⁷⁷ These results can be compared with experiment⁷⁸ and thus provide a test of some of the new techniques described in this report.

References

1. J. O. Hirschfelder, C. F. Curtiss, and R. B. Bird, "Molecular Theory of Gases and Liquids", Wiley, New York, 1954.
2. M. Mitchner and C. H. Kruger, Jr., "Partially Ionized Gases", Wiley, New York, 1973.
3. E. A. Mason and L. Monchick, J. Chem. Phys. 36, 1622 (1962).
4. E. W. McDaniel and E. A. Mason, "The Mobility and Diffusion of Ions in Gases", Wiley, New York, 1973.
5. T. E. Horton and W. A. Menard, NASA TR-32-1350, 1969.
6. J. N. Moss, E. C. Anderson, and C. W. Bolz, Jr., Paper No. 75-671, AIAA 10th Thermophys. Conf., Denver, May, 1975.
7. J. N. Moss, E. C. Anderson, and C. W. Bolz, Jr., Paper No. 76-469, AIAA 11th Thermophys. Conf., San Diego, July, 1976.
8. L. Biolsi, J. Geophys. Res. 83, 1125 (1978).
9. T. Kihara, M. H. Taylor, and J. O. Hirschfelder, Phys. Fluids 3, 715 (1960).
10. E. A. Mason, J. Chem. Phys. 22, 169 (1954).
11. F. J. Smith and R. J. Munn, J. Chem. Phys. 41, 3560 (1964).
12. L. Monchick, Phys. Fluids 2, 695 (1959).
13. A. Dalgarno and N. Lynn, Proc. Phys. Soc. (London) A 69, 821 (1956).
14. E. A. Mason and W. E. Rice, J. Chem. Phys. 22, 522 (1954).
15. R. A. Buckingham, Trans. Faraday Soc. 54, 453 (1958).
16. J. T. Vanderslice, S. Weissman, E. A. Mason, and R. J. Fallon, Phys. Fluids 5, 155 (1962).
17. D. R. Bates, K. Ledsham, and A. L. Stewart, Phil. Trans. Roy. Soc. (London) A 246, 215 (1953).
18. A. A. Evett, J. Chem. Phys. 24, 150 (1956).
19. E. A. Mason and J. T. Vanderslice, J. Chem. Phys. 29, 361 (1958).
20. H. H. Michels, J. Chem. Phys. 44, 3834 (1966).
21. R. J. Fallon, E. A. Mason, and J. T. Vanderslice, Astrophys. J. 131, 12 (1959).
22. E. A. Mason and J. T. Vanderslice, J. Chem. Phys. 27, 917 (1957).
23. E. A. Mason, R. J. Munn, and F. J. Smith, Phys. Fluids 10, 1827 (1967).
24. H. Hahn, E. A. Mason, and F. J. Smith, Phys. Fluids 14, 278 (1971).
25. H. Hahn, E. A. Mason, E. J. Miller, and S. I. Sandler, J. Plasma Phys. 7, 285 (1972).

26. R. S. Devoto, Phys. Fluids 9, 1230 (1966).
27. C. P. Li and R. S. Devoto, Phys. Fluids 11, 448 (1968).
28. W. F. Ahtye, NASA TN D-2611, 1965.
29. S. I. Sandler and E. A. Mason, Phys. Fluids 12, 71 (1969).
30. J. N. Moss, private communication.
31. L. Biolsi, J. Geophys. Res. 83, 2476 (1978).
32. G. Herzberg, "Molecular Spectra and Molecular Structure, Vol. 1, Spectra of Diatomic Molecules", Van Nostrand, Princeton, 1950.
33. E. A. Ballik and D. A. Ramsay, Astrophys. J. 137, 84 (1963).
34. P. F. Fougere and R. K. Nesbet, J. Chem. Phys. 44, 285 (1966).
35. D. R. Stull and H. Prophet (eds.), "JANAF Thermochemical Tables", NSRDS-NBS 37, 1971.
36. H. M. Hulburt and J. O. Hirschfelder, J. Chem. Phys. 9, 61 (1941).
37. H. M. Hulburt and J. O. Hirschfelder, J. Chem. Phys. 35, 1901 (1961).
38. D. Steele, E. R. Lippincott, and J. T. Vanderslice, Rev. Mod. Phys. 34, 239 (1962).
39. I. N. Levine, J. Chem. Phys. 45, 827 (1966).
40. M. Klein, H.J.M. Hanley, F. J. Smith, and P. Holland, NSRDS-NBS 47, 1974.
41. R. S. Mulliken, J. Phys. Chem. 41, 5 (1937).
42. R. Rydberg, Z Physik 80, 514 (1933).
43. O. Klein, Z. Physik 76, 226 (1932).
44. A.L.G. Rees, Proc. Phys. Soc. (London) 59, 998 (1947).
45. J. L. Dunham, Phys. Rev. 41, 721 (1932).
46. J. T. Vanderslice, E. A. Mason, W. G. Maisch, and E. R. Lippincott, J. Mol. Spec. 3, 17 (1959).
47. J. T. Vanderslice, E. A. Mason, W. G. Maisch, and E. R. Lippincott, J. Mol. Spec. 5, 83 (1960).
48. S. M. Read and J. T. Vanderslice, J. Chem. Phys. 36, 2366 (1962).
49. C. A. Coulson, "Valence", Oxford University Press, New York, 1952.
50. J. T. Vanderslice, E. A. Mason, and E. R. Lippincott, J. Chem. Phys. 30, 129 (1959).
51. J. T. Vanderslice, E. A. Mason, and W. G. Maisch, J. Chem. Phys. 32, 515 (1960).

52. L. Biolsi, NASA Semi-annual Report, Dec., 1977.
53. L. Biolsi, NASA Semi-annual Report, June, 1978.
54. J. M. Yos, Tech. Memo. RAD-TM-63-7, AVCO Corp., Boston, 1963.
55. E. Clementi, *Astrophys. J.* 133, 303 (1961).
56. L. Biolsi, Paper No. 78-906, 2nd AIAA/ASME Thermophys. Conf. Palo Alto, May, 1978.
57. L. Biolsi and L. R. Wallace, "Progress in Astronautics and Aeronautics" (in press).
58. K. S. Yun and E. A. Mason, *Phys. Fluids* 5, 380 (1962).
59. J. T. Vanderslice, E. A. Mason, W. G. Maisch, and E. R. Lippincott, *J. Chem. Phys.* 33, 614 (1960).
60. G. C. Lie and J. Hinze, *J. Chem. Phys.* 59, 1872 (1973).
61. H.P.D. Liu and G. Verhaegen, *J. Chem. Phys.* 53, 735 (1970).
62. W. M. Huo, *J. Chem. Phys.* 43, 624 (1965).
63. H. F. Schaefer III and F. E. Harris, *J. Chem. Phys.* 48, 4946 (1968).
64. R. K. Lengel and D. R. Crosley, *J. Chem. Phys.* 67, 2085 (1977).
65. E. A. Mason and W. E. Rice, *J. Chem. Phys.* 22, 843 (1954).
66. I. Amdur, E. A. Mason, and J. E. Jordan, *J. Chem. Phys.* 27, 527 (1957).
67. I. Amdur, M. S. Longmire, and E. A. Mason, *J. Chem. Phys.* 35, 895 (1961).
68. M. Cowperthwaite and S. H. Bauer, *J. Chem. Phys.* 36, 1743 (1962).
69. W. Klemperer, *Nature* 227, 1230 (1970).
70. I. Amdur, W. A. Peters, J. E. Jordan, and E. A. Mason, *J. Chem. Phys.* 64, 1538 (1976).
71. I. Amdur, M. S. Longmire, J. E. Jordan, and E. A. Mason, *J. Chem. Phys.* 63, 2926 (1975).
72. D. D. Esch, A. Siripong, and R. W. Pike, NASA CR-111989, 1970.
73. C.R.A. Catlow, A. H. Harker, and M. R. Hayns, *J. Chem. Soc. Faraday Trans. II* 71, 275 (1975).
74. E. A. Mason, J. T. Vanderslice, and J. M. Yos, *Phys. Fluids* 2, 688 (1959).
75. P. H. Krupenie, *J. Phys. Chem. Ref. Data*, Vol. 1 2, 423 (1972).
76. R. N. Dixon and C. Thomson (eds.), "Theoretical Chemistry Volume 2", Bartholomew Press, Dorking, England, 1975.
77. K. S. Yun, S. Weissman, and E. A. Mason, *Phys. Fluids* 5, 672 (1962).
78. J. Hilsenrath, C. W. Beckett, W. S. Benedict, L. Fano, H. J. Hoge, J. F. Masi, R. L. Nuttall, Y. S. Touloukian, and H. W. Woolley, NBS Circ. No. 564 (1955).

Table 1

Mole Fractions of Species in the Jovian Atmosphere as a Function
of Temperature at 1 Atmosphere Pressure

$T \times 10^{-3} (^{\circ}\text{K})$	H_2	H	He	H^+	He^+	e
1	0.8900		0.1100			
2	0.8854	0.0015	0.1099			
3	0.7596	0.1380	0.1024			
4	0.2054	0.7245	0.0702			
5	0.0203	0.9204	0.0594			
6	0.0032	0.9383	0.0584			
7	0.0008	0.9400	0.0582	0.0005		0.0005
8	0.0003	0.9372	0.0581	0.0022		0.0022
9	0.0001	0.9269	0.0578	0.0076		0.0076
10	0.0001	0.9019	0.0570	0.0205		0.0205
11		0.8525	0.0555	0.0460		0.0460
12		0.7699	0.0531	0.0885		0.0885
13		0.6522	0.0495	0.1492		0.1492
14		0.5091	0.0452	0.2228		0.2228
15		0.3629	0.0408	0.2981		0.2981
16		0.2378	0.0370	0.3625	0.0001	0.3626
17		0.1469	0.0342	0.4093	0.0002	0.4095
18		0.0885	0.0321	0.4392	0.0005	0.4397
19		0.0535	0.0302	0.4568	0.0013	0.4581
20		0.0307	0.0280	0.4666	0.0028	0.4694
21		0.0211	0.0249	0.4715	0.0055	0.4770
22		0.0140	0.0207	0.4733	0.0094	0.4827
23		0.0095	0.0158	0.4733	0.0140	0.4873
24		0.0067	0.0112	0.4726	0.0184	0.4910
25		0.0049	0.0076	0.4719	0.0219	0.4938

Table 2

Interaction Potentials in the Jovian Atmosphere

Inter- action	Poten- tial	Refer- ences (ab initio results)	Refer- ences (para- meters)	Temp. (°K)	Parameters		
H-H ($^1\Sigma$)	AIP	13	16	low	A=37.97	B=6	
	AIP	13	16	high	A=12.43	B=4.36	
H-H ($^3\Sigma$)	ER	13	16	all	F=60.42	D=3.013	
He-He	ES	14	14	1000	$\alpha=12.4$	$r_e=3.135$	$\epsilon/k=9.16$
	ER	15	21	2000-10,000	F=384.1	D=4.502	
	ER	15	21	>10,000	F=44.79	D=2.903	
H ₂ -H ₂	ES	14	14	≤ 7000	$\alpha=14.0$	$r_e=3.337$	$\epsilon/k=37.3$
	ER	16	16	>7000	F=116.5	D=2.859	
H ₂ -H	ER	16	16	all	F=61.5	D=2.952	
H ₂ -He	ES	14	14	≤ 3000	$\alpha=13.22$	$r_e=3.244$	$\epsilon/k=18.27$
	ER		8	>3000	F=211.5	D=3.699	
H-He	ER	15	21	all	F=74.73	D=3.159	
H-H ⁺ ($2p_\sigma$)	ER	17	21	all	F=56.38	D=1.719	
H-H ⁺ ($1s_\sigma$)	MP	17	8	all	C=1.230	$r_e=1.100$	$\epsilon=2.800$
He-H ⁺	MP	18	22	all	C=1.230	$r_e=0.762$	$\epsilon=1.905$
He-He ⁺ ($^2\Sigma_u$)	MP	19	19	all	C=1.637	$r_e=1.080$	$\epsilon=2.16$
He-He ⁺ ($^2\Sigma_g$)	ER	19	19	all	F=44.40	D=2.157	
H-He ⁺ ($^1\Sigma$)	ER	20	8	all	F=149.2	D=3.019	
H-He ⁺ ($^3\Sigma$)	ER	20	8	all	F=157.75	D=3.716	

The parameters have been chosen so that $V(r)$ is in electron volts and r is in Angstroms.

Table 3
Collision Integrals for the H-H Interaction

$T \times 10^{-3} \text{ (}^\circ\text{K)}$	$\sigma_{\Omega}^2(1,1)^* \text{ (}\text{\AA}^2\text{)}$	$\sigma_{\Omega}^2(2,2)^* \text{ (}\text{\AA}^2\text{)}$
1	5.235	5.954
2	4.133	4.743
3	3.570	4.118
4	3.230	3.742
5	3.028	3.500
6	2.884	3.281
7	2.760	3.063
8	2.622	2.883
9	2.479	2.730
10	2.356	2.598
11	2.249	2.483
12	2.154	2.380
13	2.070	2.289
14	1.993	2.205
15	1.924	2.130
15.5	1.890	2.093
16	1.858	2.058
16.5	1.829	2.026
17	1.801	1.995
17.5	1.773	1.964
18	1.746	1.934
19	1.699	1.882
20	1.653	1.833
21	1.610	1.785
22	1.569	1.738
23	1.532	1.697
24	1.496	1.658
25	1.463	1.620

Table 4
Collision Integrals for the He-He Interaction

$T \times 10^{-3} \text{ (}^\circ\text{K)}$	$\sigma_{\Omega}^2(1,1)^* \text{ (}\text{\AA}^2\text{)}$	$\sigma_{\Omega}^2(2,2)^* \text{ (}\text{\AA}^2\text{)}$
1	3.023	3.779
2	2.508	3.034
3	2.231	2.719
4	2.050	2.507
5	1.911	2.351
6	1.803	2.227
7	1.717	2.126
8	1.637	2.035
9	1.577	1.964
10	1.517	1.894
11	1.345	1.785
12	1.277	1.700
13	1.218	1.625
14	1.160	1.552
15	1.118	1.529
15.5	1.111	1.515
16	1.104	1.501
16.5	1.086	1.481
17	1.069	1.461
17.5	1.052	1.442
18	1.036	1.423
19	1.006	1.387
20	0.978	1.354
21	0.951	1.323
22	0.926	1.294
23	0.903	1.265
24	0.880	1.239
25	0.859	1.213

Table 5
Collision Integrals for the H_2-H_2 Interaction

$T \times 10^{-3} \text{ (}^\circ\text{K)}$	$\sigma_{\Omega}^{2(1,1)*} \text{ (}\text{\AA}^2\text{)}$	$\sigma_{\Omega}^{2(2,2)*} \text{ (}\text{\AA}^2\text{)}$
1	5.210	6.002
2	4.367	5.328
3	3.794	4.732
4	3.419	4.293
5	3.142	3.966
6	2.925	3.710
7	2.747	3.497

Table 6

Collision Integrals for the H₂-H Interaction

$T \times 10^{-3} \text{ (}^\circ\text{K)}$	$\sigma_{\Omega}^{2(1,1)*} \text{ (}\text{\AA}^2\text{)}$	$\sigma_{\Omega}^{2(2,2)*} \text{ (}\text{\AA}^2\text{)}$	A^*	B^*
1	4.157	5.134	1.235	1.200
2	3.270	4.100	1.254	1.222
3	2.802	3.549	1.266	1.237
4	2.492	3.180	1.276	1.249
5	2.265	2.907	1.284	1.259
6	2.088	2.694	1.290	1.268
7	1.943	2.518	1.296	1.276

Table 7

Collision Integrals for the H₂-He Interaction

$T \times 10^{-3} \text{ (}^\circ\text{K)}$	$\sigma_{\Omega}^2(1,1)^* \text{ (}\text{\AA}^2\text{)}$	$\sigma_{\Omega}^2(2,2)^* \text{ (}\text{\AA}^2\text{)}$	A^*	B^*
1	4.059	4.829	1.189	0.911
2	3.517	4.292	1.220	0.931
3	3.244	4.041	1.246	0.937
4	2.511	3.111	1.239	1.204
5	2.329	2.899	1.245	1.211
6	2.178	2.723	1.250	1.250
7	2.062	2.587	1.254	1.223

Table 8

Collision Integrals for the H-He Interaction

$T \times 10^{-3} \text{ (}^\circ\text{K)}$	$\sigma_{\Omega}^{2(1,1)*} \text{ (}\text{\AA}^2\text{)}$	$\sigma_{\Omega}^{2(2,2)*} \text{ (}\text{\AA}^2\text{)}$	A^*	B^*
1	3.858	4.747	1.231	1.194
2	3.050	3.809	1.249	1.215
3	2.632	3.318	1.261	1.230
4	2.349	2.983	1.270	1.241
5	2.145	2.740	1.277	1.251
6	1.977	2.538	1.284	1.259
7	1.849	2.384	1.289	1.266
8	1.742	2.254	1.294	1.273
9	1.646	2.137	1.298	1.279
10	1.560	2.033	1.303	1.285
11	1.492	1.949	1.306	1.291
12	1.425	1.867	1.310	1.296
13	1.368	1.796	1.313	1.301
14	1.318	1.734	1.316	1.305
15	1.269	1.674	1.319	1.309
15.5	1.245	1.644	1.321	1.312
16	1.222	1.615	1.322	1.314
16.5	1.202	1.589	1.323	1.316
17	1.182	1.565	1.324	1.318
17.5	1.165	1.544	1.325	1.320
18	1.149	1.524	1.326	1.321
19	1.110	1.475	1.329	1.326
20	1.078	1.435	1.331	1.329
21	1.047	1.396	1.333	1.333
22	1.016	1.357	1.336	1.336
23	0.992	1.326	1.337	1.337
24	0.968	1.296	1.339	1.342
25	0.944	1.266	1.341	1.345

Table 9

Collision Integrals for the $H-H^+$ Interaction

$T \times 10^{-3} \text{ (}^\circ K)$	$\sigma_{\Omega}^2(1,1)^* \text{ (}\text{\AA}^2)$	$\sigma_{\Omega}^2(2,2)^* \text{ (}\text{\AA}^2)$	A^*	B^*
8	30.9	6.49	0.210	1.38
9	30.4	6.02	0.198	1.38
10	30.0	5.61	0.187	1.38
11	29.6	5.28	0.178	1.37
12	29.2	4.98	0.170	1.37
13	28.9	4.74	0.164	1.37
14	28.6	4.51	0.158	1.37
15	28.3	4.31	0.152	1.37
15.5	28.2	4.21	0.149	1.37
16	28.1	4.12	0.147	1.37
16.5	27.9	4.03	0.144	1.37
17	27.8	3.95	0.142	1.37
17.5	27.7	3.87	0.139	1.37
18	27.6	3.79	0.137	1.37
19	27.4	3.66	0.134	1.37
20	27.2	3.53	0.130	1.37
21	27.0	3.42	0.127	1.37
22	26.8	3.31	0.123	1.37
23	26.6	3.21	0.120	1.37
24	26.5	3.11	0.117	1.36
25	26.3	3.02	0.115	1.36

Table 10

Collision Integrals for the H-e Interaction

$T \times 10^{-3} \text{ (}^\circ\text{K)}$	$\sigma_{\Omega}^2(1,i)^* \text{ (}\text{\AA}^2\text{)}$	$\sigma_{\Omega}^2(2,2)^* \text{ (}\text{\AA}^2\text{)}$	A^*	B^*
8	6.44	8.34	1.30	-1.73
9	6.13	7.92	1.29	-1.79
10	5.87	7.56	1.29	-1.84
11	5.63	7.24	1.29	-1.88
12	5.42	6.96	1.28	-1.92
13	5.24	6.71	1.28	-1.96
14	5.07	6.49	1.28	-1.99
15	4.92	6.29	1.28	-2.03
15.5	4.85	6.19	1.28	-2.04
16	4.78	6.10	1.28	-2.05
16.5	4.71	6.01	1.28	-2.07
17	4.65	5.93	1.28	-2.08
17.5	4.59	5.85	1.27	-2.10
18	4.53	5.77	1.27	-2.11
19	4.42	5.63	1.27	-2.14
20	4.32	5.50	1.27	-2.15
21	4.22	5.37	1.27	-2.18
22	4.14	5.25	1.27	-2.20
23	4.05	5.14	1.27	-2.22
24	3.97	5.04	1.27	-2.25
25	3.90	4.94	1.27	-2.26

Table 11

Collision Integrals for the He-H⁺ Interaction

$T \times 10^{-3} \text{ (}^\circ\text{K)}$	$\sigma_{\Omega}^{2(1,1)*} (\text{\AA}^2)$	$\sigma_{\Omega}^{2(2,2)*} (\text{\AA}^2)$	A^*	B^*
8	1.923	2.214	1.207	1.432
9	1.706	2.014	1.181	1.422
10	1.535	1.842	1.200	1.412
11	1.397	1.699	1.216	1.403
12	1.280	1.577	1.233	1.394
13	1.181	1.474	1.248	1.386
14	1.098	1.384	1.261	1.379
15	1.024	1.305	1.275	1.372
15.5	0.9906	1.269	1.282	1.369
16	0.9593	1.235	1.288	1.366
16.5	0.9307	1.203	1.293	1.363
17	0.9037	1.173	1.298	1.360
17.5	0.8777	1.114	1.304	1.357
18	0.8531	1.117	1.310	1.355
19	0.8079	1.067	1.321	1.350
20	0.7680	1.022	1.331	1.345
21	0.7312	0.9802	1.340	1.340
22	0.6977	0.9422	1.350	1.337
23	0.6678	0.9072	1.359	1.341
24	0.6397	0.8752	1.368	1.345
25	0.6141	0.8450	1.376	1.349

Table 12

Collision Integrals for the He-e Interaction

$T \times 10^{-3} \text{ (}^\circ\text{K)}$	$\sigma_{\Omega}^{2(1,1)*} \text{ (}\text{\AA}^2\text{)}$
8	2.625
9	2.629
10	2.632
11	2.632
12	2.630
13	2.627
14	2.623
15	2.620
15.5	2.617
16	2.615
16.5	2.613
17	2.611
17.5	2.608
18	2.606
19	2.595
20	2.585
21	2.578
22	2.567
23	2.554
24	2.544
25	2.483

$$\sigma_{\Omega}^{2(2,2)*} = \sigma_{\Omega}^{2(1,1)*}$$

$A^* = B^* = 1$ for all values of T

Table 13

Collision Integrals for the H^+-H^+ , He^+-He^+ , and H^+-He^+ Interactions

$T \times 10^{-3} \text{ (}^\circ K)$	$\lambda_d^{2\Omega}(1,1)^* \text{ (}\text{\AA}^2)$	$\lambda_d^{2\Omega}(2,2)^* \text{ (}\text{\AA}^2)$	A^*	B^*
8	845.11	960.46	1.1365	1.1735
9	596.71	685.89	1.1495	1.1892
10	445.79	517.35	1.1605	1.2026
11	343.68	402.01	1.1698	1.2136
12	272.11	320.73	1.1765	1.2215
13	224.96	266.37	1.1809	1.2268
14	191.57	226.67	1.1832	1.2295
15	165.37	195.75	1.1837	1.2301
15.5	155.96	184.50	1.1830	1.2292
16	147.37	174.23	1.1823	1.2284
16.5	139.88	165.19	1.1809	1.2268
17	132.98	156.86	1.1796	1.2252
17.5	127.17	149.78	1.1778	1.2231
18	121.77	143.21	1.1760	1.2210
19	113.26	132.74	1.1720	1.2162
20	105.03	122.67	1.1680	1.2115
21	98.400	114.54	1.1641	1.2069
22	91.607	106.31	1.1605	1.2026
23	85.709	99.192	1.1574	1.1988
24	81.103	93.610	1.1542	1.1950
25	76.319	87.863	1.1513	1.1914

The values of A^* and B^* can be taken to be unity at all values of T for the H^+-H^+ and He^+-He^+ interactions.

Table 14
Collision Integrals for the e-e Interaction

$T \times 10^{-3} \text{ (}^\circ\text{K)}$	$\lambda_d^{2\Omega}(1,1)^* \text{ (}\text{\AA}^2\text{)}$	$\lambda_d^{2\Omega}(2,2)^* \text{ (}\text{\AA}^2\text{)}$
8	841.70	952.55
9	593.73	678.84
10	443.11	510.91
11	341.26	396.01
12	269.90	315.28
13	222.91	261.27
14	189.67	221.88
15	163.61	191.22
15.5	154.27	180.11
16	145.73	169.96
16.5	138.29	161.04
17	131.44	152.83
17.5	125.68	145.86
18	120.32	139.40
19	111.89	129.11
20	103.74	119.22
21	97.174	111.25
22	90.438	103.17
23	84.595	96.190
24	80.036	90.718
25	75.302	85.097

Table 15

Collision Integrals for the H^+-e and He^+-e Interactions

$T \times 10^{-3} \text{ (}^\circ K)$	$\lambda_d^2 \Omega^{(1,1)*} \text{ (}\text{\AA}^2)$	$\lambda_d^2 \Omega^{(2,2)*} \text{ (}\text{\AA}^2)$	A^*	B^*
8	881.11	967.49	1.0980	1.2866
9	631.96	696.15	1.1016	1.3030
10	478.96	528.84	1.1041	1.3168
11	374.08	413.57	1.1056	1.3300
12	299.66	331.47	1.1061	1.3384
13	249.52	276.10	1.1065	1.3422
14	212.58	235.21	1.1065	1.3433
15	183.61	203.12	1.1062	1.3458
15.5	172.50	191.29	1.1089	1.3484
16	162.39	180.49	1.1115	1.3510
16.5	153.78	170.89	1.1113	1.3499
17	145.87	162.07	1.1111	1.3488
17.5	139.09	154.50	1.1108	1.3467
18	132.80	147.48	1.1106	1.3446
19	122.72	136.22	1.1100	1.3385
20	113.07	125.44	1.1094	1.3337
21	105.30	116.75	1.1087	1.3278
22	97.519	108.04	1.1079	1.3245
23	90.819	100.55	1.1071	1.3224
24	85.546	94.648	1.1064	1.3179
25	80.173	88.640	1.1056	1.3142

Table 16

Collision Integrals for the H-He⁺ Interaction

$T \times 10^{-3} \text{ (}^\circ\text{K)}$	$\sigma_{\Omega}^{2(1,1)*} (\text{\AA}^2)$	$\sigma_{\Omega}^{2(2,2)*} (\text{\AA}^2)$	A^*	B^*
15	1.483	1.904	1.283	1.266
15.5	1.461	1.877	1.284	1.268
16	1.440	1.852	1.286	1.270
16.5	1.420	1.828	1.287	1.272
17	1.401	1.805	1.288	1.274
17.5	1.382	1.782	1.289	1.275
18	1.364	1.760	1.290	1.277
19	1.329	1.719	1.293	1.280
20	1.298	1.680	1.294	1.283
21	1.266	1.642	1.297	1.286
22	1.237	1.606	1.298	1.288
23	1.210	1.573	1.300	1.291
24	1.183	1.539	1.301	1.294
25	1.158	1.510	1.304	1.296

Table 17

Collision Integrals for the He-He⁺ Interaction

$T \times 10^{-3} \text{ (}^\circ\text{K)}$	$\sigma_{\Omega}^{2(1,1)*} (\text{\AA}^2)$	$\sigma_{\Omega}^{2(2,2)*} (\text{\AA}^2)$	A^*	B^*
15	91.7	2.69	0.030	1.37
15.5	91.9	2.63	0.029	1.37
16	92.1	2.57	0.029	1.37
16.5	92.2	2.52	0.028	1.37
17	92.4	2.47	0.027	1.37
17.5	92.6	2.42	0.027	1.37
18	92.9	2.37	0.026	1.37
19	93.2	2.29	0.025	1.38
20	93.4	2.22	0.024	1.38
21	93.6	2.14	0.023	1.38
22	93.9	2.07	0.022	1.38
23	94.1	2.01	0.021	1.38
24	94.3	1.96	0.021	1.38
25	94.5	1.90	0.020	1.38

Table 18
The He-H⁺ Interaction Potential as a Function of Internuclear
Separation

<u>r (Å)</u>	<u>V_{ab initio} (ev)²²</u>	<u>V_{Morse} (ev)</u>
0.5290	0.29	-0.69
0.6348	-1.54	-1.63
0.7406	-1.90	-1.90
0.8464	-1.84	-1.83
0.9522	-1.66	-1.63
1.1638	-1.28	-1.13
1.2696	-1.12	-0.91
1.3754	-0.99	-0.72
1.4812	-0.88	-0.57
1.5870	-0.78	-0.45
1.6928	-0.48	-0.35
1.7986	-0.36	-0.27
1.9044	-0.27	-0.21
2.0102	-0.20	-0.16
2.1160	-0.16	-0.12
2.2218	-0.12	-0.09
2.3276	-0.10	-0.07

Table 19

Mole Fractions of Neutral Carbon Species as a Function of Temperature
and Distance From the Stagnation Point

<u>Distance (cm)</u>	<u>T (°K)</u>	<u>X (C)</u>	<u>X (C₂)</u>	<u>X (C₃)</u>
0.00	4268	0.0258	0.0275	0.3034
0.05	4633	0.0724	0.0558	0.3368
0.10	5141	0.2075	0.0971	0.2631
0.15	5553	0.3870	0.1175	0.1466
0.20	5855	0.5236	0.1211	0.0487
0.24	6236	0.6367	0.0937	0.0081
0.27	6601	0.6662	0.0571	0.0013
0.29	7775	0.6534	0.0098	
0.32	9790	0.5006	0.0008	
0.33	10,742	0.3992	0.0002	
0.34	11,424	0.3076	0.0001	
0.35	11,980	0.2300		
0.37	12,456	0.1692		
0.38	12,821	0.1217		
0.39	13,170	0.0857		
0.40	13,392	0.0609		
0.42	13,598	0.0429		
0.43	13,773	0.0302		
0.44	13,931	0.0211		
0.45	14,058	0.0147		
0.46	14,169	0.0102		
0.49	14,344	0.0046		
0.51	14,487	0.0018		
0.54	14,614	0.0006		

Table 20

Interaction Potential Parameters for the $C(^3P)-C(^3P)$ Interaction

State	Potential	Parameters*		
$1\Sigma_g^+$	MP	$C=2.500$	$r_e=1.2420$	$\epsilon=6.36$
$1\Pi_u$	MP	$C=2.193$	$r_e=1.3119$	$\epsilon=6.28$
$3\Sigma_g^-$	MP	$C=2.182$	$r_e=1.3692$	$\epsilon=5.59$
$1\Pi_u$	MP	$C=2.339$	$r_e=1.3184$	$\epsilon=5.33$
$3\Sigma_u^+$	MP	$C=2.997$	$r_e=1.23$	$\epsilon=4.70$
$1\Delta_g$	MP	$C=2.697$	$r_e=1.39$	$\epsilon=4.45$
$1\Sigma_g^{+2}$	MP	$C=2.238$	$r_e=1.38$	$\epsilon=4.03$
$3\Pi_g$	MP	$C=2.978$	$r_e=1.2660$	$\epsilon=3.89$
$5\Pi_g$	MP	$C=2.739$	$r_e=1.46$	$\epsilon=3.54$
$5\Sigma_g^+$	MP	$C=4.044$	$r_e=1.35$	$\epsilon=2.55$
$1\Pi_g$	MP	$C=4.328$	$r_e=1.2552$	$\epsilon=2.11$
$3\Delta_u$	MP	$C=4.071$	$r_e=1.51$	$\epsilon=2.02$
$1\Sigma_u^-$	MP	$C=3.474$	$r_e=1.90$	$\epsilon=1.98$
$5\Sigma_u^-$	ER	$F=309.5$	$D=0.4060$	
$5\Pi_u$	ER	$F=400.0$	$D=0.3601$	
$5\Delta_g$	ER	$F=504.3$	$D=0.3931$	
$3\Sigma_u^{+2}$				
$5\Sigma_g^{+2}$				

*The parameters have been chosen so that $V(r)$ is in electron volts and r is in Angstroms.

Table 21

Transport Collision Integrals for the $C(^3P)-C(^3P)$ Interaction

$T \times 10^{-3} (^{\circ}K)$	$\sigma_{\Omega}^{2(1,1)*} (A^2)$	$\sigma_{\Omega}^{2(2,2)*} (A^2)$
1	10.4254	10.9550
2	8.9651	9.3214
3	8.1203	8.4021
4	7.5021	7.7863
5	7.0400	7.3393
6	6.6325	6.9795
7	6.2860	6.6854
8	5.9865	6.4239
9	5.6957	6.1864
10	5.4336	5.9610
11	5.2017	5.7595
12	4.9823	5.5740
13	4.7842	5.3833
14	4.6072	5.2186
15	4.4449	5.0620
16	4.2958	4.9137
17	4.1499	4.7715
18	4.0144	4.6372
19	3.8860	4.4885
20	3.7654	4.3663
21	3.6374	4.2454
22	3.5324	4.1436
23	3.4366	4.0423
24	3.3474	3.9462
25	3.2630	3.8553

Table 22

Potential Energy Curves for the Hulburt-Hirschfelder
 Potential and the Morse Potential for the $1\Sigma_g^+$ State of C_2

<u>r (Å)</u>	<u>V_{HH} (ev)</u>	<u>V_{Morse} (eV)</u>
1.058	-4.42	-4.83
1.111	-5.49	-5.67
1.242	-6.36	-6.36
1.323	-6.15	-6.19
1.429	-5.47	-5.65
1.588	-4.15	-4.59
1.852	-2.26	-2.94
2.117	-1.13	-1.76
2.646	-0.29	-0.59
3.704	-0.03	-0.06
5.292	0	0

Table 23
The Hulburt-Hirschfelder Potential for the $^1\Pi_g$ State of C_2

r/σ	$V(r)/\epsilon$
1.150	-0.996
1.300	-0.560
1.450	-0.115
1.600	0.036
1.750	0.042
1.900	0.021
2.050	0.007
2.200	0.001
2.350	0
2.500	-0.001
2.650	0

Table 24

Comparison of the Collision Integrals for the $1\Sigma_g^+$ State of C_2
for the Hulburt-Hirschfelder and Morse Potentials

$T \times 10^{-3}$ ($^{\circ}K$)	$\sigma_{\Omega}^{2(1,1)*}$ (HH)	$\sigma_{\Omega}^{2(1,1)*}$ (MP)	$\sigma_{\Omega}^{2(2,2)*}$ (HH)	$\sigma_{\Omega}^{2(2,2)*}$ (MP)
1	7.4841	11.6132	7.8147	11.5269
2	6.4250	10.1956	6.5837	9.7526
3	5.8522	9.3141	5.9310	8.8155
4	4.6151	8.7405	4.6097	8.2219
5	4.4527	8.2450	4.4743	7.7398
6	4.3244	7.8490	4.3666	7.3881
7	4.2186	7.5016	4.2777	7.0946
8	4.1288	7.2046	4.2017	6.8832
9	4.0513	6.8877	4.1359	6.6577
10	3.9835	6.6343	4.0782	6.4829
11	3.9231	6.3719	4.0267	6.3035
12	3.8686	6.1279	3.9801	6.1357
13	3.8192	5.9332	3.9378	5.9996
14	3.7735	5.7057	3.8965	5.8370
15	3.7144	5.5028	3.8505	5.7879
16	3.6084	5.3264	3.7702	5.5547
17	3.5102	5.1482	3.6951	5.4163
18	3.4208	4.9687	3.6264	5.2730
19	3.3382	4.8185	3.5624	5.1498
20	3.2620	4.6680	3.5030	5.0234
21	3.1905	4.5177	3.4469	4.8940
22	3.1233	4.3678	3.3939	4.7620
23	3.0480	4.2188	3.3284	4.6277
24	2.9740	4.1004	3.2630	4.5188
25	2.9069	3.9829	3.2033	4.4090

The collision integrals are given in units of (Angstroms)².

Table 25

RKR and Hulburt-Hirschfelder Potential Energy Results

for the $1\Sigma_g^+$, $3\Pi_u$, and $1\Pi_g$ States of C_2

$1\Sigma_g^+$			$3\Pi_u$			$1\Pi_g$		
r (Å)	V (RKR)	V (HH)	r (Å)	V (RKR)	V (HH)	r (Å)	V (RKR)	V (HH)
1.134	0.564	0.564	1.098	2.149	2.164	1.103	1.201	1.377
1.156	0.341	0.342	1.105	1.977	1.993	1.111	1.078	1.187
1.190	0.115	0.117	1.113	1.802	1.808	1.120	0.922	1.001
1.301	0.115	0.115	1.121	1.525	1.635	1.132	0.740	0.790
1.349	0.341	0.344	1.131	1.445	1.435	1.148	0.541	0.563
1.384	0.564	0.564	1.141	1.262	1.253	1.169	0.330	0.341
			1.152	1.076	1.070	1.202	0.112	0.119
			1.164	0.886	0.891	1.313	0.112	0.109
			1.179	0.695	0.696	1.365	0.330	0.344
			1.197	0.500	0.500	1.405	0.540	0.575
			1.221	0.302	0.297	1.444	0.740	0.815
			1.257	0.101	0.100	1.488	0.922	1.083
			1.374	0.101	0.101	1.545	1.078	1.398
			1.425	0.302	0.303	1.621	1.201	1.729
			1.463	0.500	0.501			
			1.495	0.695	0.692			
			1.525	0.886	0.852			
			1.553	1.076	1.073			
			1.580	1.262	1.260			
			1.605	1.445	1.437			
			1.630	1.625	1.615			
			1.655	1.802	1.793			
			1.679	1.977	1.964			
			1.702	2.149	2.127			

Potential energy is given in electron volts.

Table 26

Molecular Orbital Arrangements for the ${}^3\Sigma_u^+$, ${}^5\Pi_g^+$, ${}^3\Sigma_u$, and ${}^3\Sigma_g^-$ States of C_2 According to the Perfect Pairing Method

<u>Molecular Orbital</u>	<u>${}^3\Sigma_u^+$</u>	<u>${}^5\Sigma_g^+$</u>	<u>${}^3\Pi_u$</u>	<u>${}^3\Sigma_g^-$</u>
σ_u^*2p	\uparrow			
$\Pi_g^{*-}2p$		\uparrow		
$\Pi_g^{*+}2p$		\uparrow		
Π_u^-2p	\downarrow	\uparrow	\uparrow	\uparrow
Π_u^+2p	\uparrow	\uparrow	$\uparrow\downarrow$	\uparrow
σ_g2p	\uparrow		\uparrow	$\uparrow\downarrow$

For each state, eight electrons fill the molecular orbitals

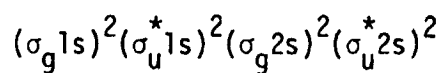


Table 27
 Potential Energy Curves for the $^3\Sigma_u^+$ and $^5\Sigma_g^+$ States of C_2
 Obtained by the Perfect Pairing Method

r (Å)	V ($^3\Sigma_u^+$)	V ($^5\Sigma_g^+$)
1.80		3.38
1.85		3.04
1.90		2.70
1.95		2.40
2.00		2.14
2.05		1.90
2.10	0.44	1.68
2.15	0.42	1.50
2.20	0.42	1.32
2.25	0.42	1.16
2.30	0.40	1.02
2.35	0.38	0.90
2.40	0.36	0.80
2.45	0.36	0.70
2.50	0.34	0.62
2.55	0.30	0.56
2.60	0.28	0.50
2.65	0.26	0.44
2.70	0.24	0.38
2.75	0.22	0.34
2.80	0.22	0.30
2.85	0.20	0.26
2.90	0.18	0.24
2.95	0.16	0.22
3.00	0.16	0.18

The potential energy is in electron volts.

Table 28

Mole Fraction of Carbon Atoms in the Three Lowest Electronic States

$T \times 10^{-3} (^{\circ}\text{K})$	$x (^3\text{P})$	$x (^1\text{D})$	$x (^1\text{S})$
1	1.00	0.00	0.00
2	1.00	0.00	0.00
3	1.00	0.00	0.00
4	0.99	0.01	0.00
5	0.97	0.03	0.00
6	0.95	0.05	0.00
7	0.94	0.06	0.00
8	0.92	0.08	0.00
9	0.90	0.10	0.00
10	0.88	0.11	0.00
11	0.86	0.13	0.01
12	0.84	0.14	0.01
13	0.82	0.15	0.01
14	0.80	0.16	0.01
15	0.78	0.16	0.01
16	0.76	0.17	0.01
17	0.73	0.17	0.01
18	0.71	0.17	0.01
19	0.68	0.17	0.02
20	0.65	0.17	0.02
21	0.61	0.17	0.02
22	0.58	0.17	0.02
23	0.55	0.16	0.02
24	0.52	0.16	0.02
25	0.49	0.15	0.02

Table 29

Spectroscopic Constants for the States of C_2 that Dissociate into
a 3P Carbon Atom and a 1D Carbon Atom

State	g_i	ϵ (e.v.)	r_e (Å)	ω_e	$\omega_e x_e$	B_e	α_e
$^3\Phi_g$	6	2.88	1.53	1290	9.0	1.20	0.011
$^3\Pi_{g2}$	6	2.56	1.535	1107	39.26	1.1922	0.0242
$^3\Delta_{u2}$	6	2.55	1.51	1380	9.2	1.23	0.011
$^3\Pi_{g3}$	6	2.35	1.49	1340	9.5	1.265	0.012
$^3\Sigma^+_{u3}$	3	2.25	1.44	1660	10.2	1.355	0.011
$^3\Pi_{u2}$	6	2.08	2.31	1000			
$^3\Phi_u$	6						
$^3\Delta_g$	6						
$^3\Sigma^+_g$	3						
$^3\Sigma^-_u$	3						
$^3\Delta_{u3}$	6						
$^3\Delta_{g2}$	6						
$^3\Pi_{u3}$	6						
$^3\Pi_{g4}$	6						
$^3\Pi_{u4}$	6						
$^3\Sigma^-_g$	3						
$^3\Sigma^-_{u2}$	3						
$^3\Sigma^-_{g2}$	3						

The constants ω_e , $\omega_e x_e$, B_e and α_e are in cm^{-1} .

Table 30

Interaction Potential Parameters for the $C(^3P)-C(^1D)$ Interaction

State	Potential	Parameters		
$^3\phi_g$	MP	$C=3.1319$		
$^3\Pi_{g2}$	MP	$C=2.6543$		
$^3\Delta_{u2}$	MP	$C=4.4409$		
$^3\Pi_{g3}$	MP	$C=3.4789$		
$^3\Sigma_u^+$	MP	$C=6.2189$		
$^3\Pi_{u2}$	MP	$C=2.3878$		
$^3\phi_u$	MP	$C=4.0000$	$r_e=3.5827$	$\epsilon=0.03$
$^3\Delta_g$	MP	$C=4.6451$	$r_e=3.5827$	$\epsilon=0.01$
$^3\Sigma_g^+$	ER	$F=66.35$	$D=1.0235$	
$^3\Sigma_u^-$	MP	$C=2.8790$	$r_e=2.6460$	$\epsilon=0.14$
$^3\Delta_{u3}$				
$^3\Delta_{g2}$				
$^3\Pi_{u3}$				
$^3\Pi_{g4}$				
$^3\Pi_{u4}$				
$^3\Sigma_g^-$				
$^3\Sigma_{u2}^-$				
$^3\Sigma_{g2}^-$				

The parameters have been chosen so that $V(r)$ is in electron volts and r is in Angstroms.

Table 31

Transport Collision Integrals for the $C(^3P)-C(^1D)$ Interaction

$T \times 10^{-3} \text{ (}^\circ\text{K)}$	$\sigma_{\Omega}^{2(1,1)*} \text{ (}\text{\AA}^2\text{)}$	$\sigma_{\Omega}^{2(2,2)*} \text{ (}\text{\AA}^2\text{)}$	A^*	B^*
1	13.7140	14.3641	1.0556	1.1473
2	11.3329	11.8458	1.0670	1.1661
3	10.0213	10.5703	1.0719	1.1919
4	9.0667	9.7169	1.0830	1.2247
5	8.2998	9.0545	1.0969	1.2525
6	7.6588	8.4959	1.1115	1.2768
7	7.1248	8.0121	1.1252	1.2953
8	6.6458	7.5643	1.1366	1.3058
9	6.2377	7.1695	1.1465	1.3121
10	5.8680	6.7992	1.1550	1.3147
11	5.5559	6.4815	1.1618	1.3150
12	5.2661	6.1777	1.1679	1.3131
13	5.0105	5.9048	1.1727	1.3104
14	4.7796	5.6547	1.1768	1.3065
15	4.5777	5.4332	1.1802	1.3026
16	4.3820	5.2157	1.1834	1.2987
17	4.2133	4.9193	1.1859	1.2946
18	4.0600	4.8537	1.1880	1.2905
19	3.9160	4.6999	1.1898	1.2873
20	3.7889	4.5450	1.1913	1.2825
21	3.6662	4.4043	1.1927	1.2790
22	3.5570	4.2789	1.1939	1.2762
23	3.4560	4.1620	1.1952	1.2729
24	3.3635	4.0545	1.1961	1.2699
25	3.2712	3.9530	1.1970	1.2672

Table 32

Spectroscopic Constants and Interaction Potential Parameters for the
 $C(^1D)-C(^1D)$ Interaction

State	ζ_i	ϵ (e.v.)	r_e (Å)	Morse Parameters		
$^1\phi_g$	2	3.56	1.51	C=2.7084		
$^1\pi_{g2}$	2	2.60	1.46	C=3.3321		
$^1\Sigma_{u2}^-$	1	2.49	1.45	C=4.5192		
$^1\Delta_u$	2	2.35	1.39	C=3.7762		
$^1\pi_{g3}$	2	2.07	1.45	C=4.8855		
$^1\Gamma_g$	2			C=4.3224	$r_e=3.5825$	$\epsilon=0.02$
$^1\phi_u$	2			C=4.3224	$r_e=3.5825$	$\epsilon=0.02$
$^1\Delta_g$	2					
$^1\Delta_{g2}$	2					
$^1\Sigma_g^+$	1					
$^1\Sigma_{g2}^+$	1					
$^1\Sigma_{g3}^+$	1					
$^1\pi_u$	2					
$^1\pi_{u2}$	2					
$^1\Sigma_{u3}^-$	1					

The parameters have been chosen so that $V(r)$ is in electron volts and r is in Angstroms.

Table 33
Transport Collision Integrals for the $C(^1D)-C(^1D)$ Interaction

$T \times 10^{-3} (^{\circ}K)$	$\sigma_{\Omega}^{2(1,1)*} (A^2)$	$\sigma_{\Omega}^{2(2,2)*} (A^2)$
1	8.3971	8.7779
2	6.8097	7.2654
3	5.8666	6.3915
4	5.2095	5.7754
5	4.7130	5.3022
6	4.3273	4.9241
7	4.0144	4.6035
8	3.7558	4.3456
9	3.5383	4.1189
10	3.3595	3.9293
11	3.2011	3.7598
12	3.0675	3.6151
13	2.9490	3.4860
14	2.8433	3.3701
15	2.7502	3.2661
16	2.6686	3.1772
17	2.5945	3.0952
18	2.5261	3.0190
19	2.4633	2.9492
20	2.4080	2.8881
21	2.3552	2.8293
22	2.3088	2.7773
23	2.2633	2.7266
24	2.2203	2.6784
25	2.1826	2.6363

Table 34

The Translational Contribution to the Thermal Conductivity, λ_{tr}^{mix} ($10^1 W/m/^\circ K$),
for a Mixture of 3P and 1D Carbon Atoms

$T \times 10^{-3}$ ($^\circ K$)	$X=0.00$	$X=0.25$	$X=0.50$	$X=0.75$	$X=1.00$
1	0.87	0.70	0.64	0.63	0.69
2	1.48	1.19	1.08	1.06	1.15
3	2.06	1.64	1.49	1.45	1.57
4	2.63	2.08	1.87	1.81	1.95
5	3.21	2.52	2.25	2.16	2.31
6	3.78	2.95	2.62	2.51	2.67
7	4.36	3.39	2.99	2.85	3.01
8	4.95	3.84	3.37	3.20	3.34
9	5.54	4.29	3.75	3.55	3.68
10	6.12	4.75	4.15	3.91	4.03
11	6.71	5.21	4.54	4.27	4.37
12	7.29	5.69	4.95	4.64	4.72
13	7.86	6.16	5.36	5.02	5.09
14	8.44	6.65	5.80	5.44	5.51
15	9.02	7.12	6.20	5.79	5.81
16	9.57	7.63	6.63	6.18	6.18
17	10.1	8.17	7.13	6.64	6.56
18	10.7	8.58	7.49	6.99	6.95
19	11.2	9.06	7.94	7.42	7.38
20	11.8	9.55	8.38	7.83	7.78
21	12.3	10.2	8.84	8.27	8.20
22	12.8	10.5	9.28	8.68	8.60
23	13.4	11.0	9.73	9.11	9.01
24	13.9	11.5	10.2	9.53	9.43
25	14.4	12.0	10.6	9.96	9.85

The symbol X denotes the mole fraction of 3P atoms.

Table 35

Mole Fractions of the Atmospheric and Ablative Species During Jovian
Entry for Stagnation-Point Peak Heating

<u>Species</u>	<u>Inner Boundary</u>	<u>Outer Boundary</u>
H	0.290	0.711
H ⁺		0.118
He	0.007	0.051
e	0.003	0.119
C	0.653	0.001
C ₂	0.010	
O	0.010	
CO	0.024	
C ⁺	0.003	0.001
Total	1.000	1.001

Table 36

Two Body Interactions at the Inner and Outer Mixing Boundaries

Inner BoundaryOuter Boundary

C-C

H-H

H-H

e-e

O-O

 $H^+ - H^+$

C-H

He-He

C-O

H-e

H-O

 $H - H^+$

H-He

 $e - H^+$

e-He

 $H^+ - He$

Table 37

Interaction Potential Parameters for the $O(^3P)-O(^3P)$ Interaction

State	Method	Potential	Temperatures	Parameters
$3\Sigma_g^-$	RKR	AIP	all	A=194.5 B=7.83
$1\Delta_g$	RKR,HH	AIP	all	A=123.4 B=7.89
$1\Sigma_g^+$	RKR,HH	AIP	all	A=141.6 B=8.64
$1\Sigma_u^-$	RKR,HH	ES	all	$\alpha=12$ $r_e=1.597$ $\epsilon=0.6655$
$3\Sigma_u^+$	RKR	AIP	low	A=480.6 B=11.46
		ES	high	$\alpha=12$ $r_e=1.518$ $\epsilon=0.8239$
$3\Delta_u$	RKR,HH	AIP	low	A=560.8 B=9.44
		ES	high	$\alpha=12$ $r_e=1.480$ $\epsilon=0.9157$
$3\Pi_u$	PP	ER	all	F=339 D=3.570
$1\Pi_u$				
$5\Pi_g$	PP	ER	all	F=717 D=3.565
$3\Pi_g$				
$1\Pi_g$				
$5\Sigma_u^-$	PP	ER	all	F=1057 D=3.567
$3\Sigma_2^+$				
$1\Sigma_{g2}^+$	PP	ER	all	F=1358 D=3.570
$5\Delta_g$	PP	ER	all	F=1433 D=3.565
$5\Sigma_g^+$				
$5\Sigma_{g2}^+$	PP	ER	all	F=2114 D=3.567
$5\Pi_u$	PP	ER	all	F=2455 D=3.567

The parameters have been chosen so that $V(r)$ is in electron volts and r is in Angstroms.

The symbol PP denotes the perfect pairing method.

Table 38

Transport Collision Integrals for the $O(^3P)-O(^3P)$ Interaction

$T \times 10^{-3} (^{\circ}K)$	$\sigma_{\Omega}^{2(1,1)*} (\text{\AA}^2)$	$\sigma_{\Omega}^{2(2,2)*} (\text{\AA}^2)$
1	6.193	7.182
2	5.271	6.139
3	4.746	5.567
4	4.386	5.174
5	4.117	4.876
6	3.905	4.640
7	3.727	4.438
8	3.575	4.271
9	3.442	4.118
10	3.335	3.996
11	3.236	3.883
12	3.148	3.782
13	3.068	3.692
14	2.996	3.609
15	2.931	3.534
16	2.931	3.457
17	2.881	3.401
18	2.835	3.349
19	2.792	3.300
20	2.752	3.255
21	2.714	3.212
22	2.679	3.172
23	2.645	3.134
24	2.614	3.098
25	2.584	3.064

Table 39

Interaction Potential Parameters for the C-H and H-O Interactions

<u>State</u>	<u>Potential</u>	<u>Parameters</u>
C-H ($^2\Pi$)	MP	$C=1.547$ $\epsilon=3.63$ $r_e=1.120$
C-H ($^4\Sigma$)	MP	$C=1.913$ $\epsilon=2.84$ $r_e=1.086$
C-H ($^2\Sigma$)	MP	$C=4.080$ $\epsilon=0.40$ $r_e=1.164$
C-H ($^4\Pi$)	ER	$F=194.53$ $D=0.3611$
H-O ($^2\Pi$)	MP	$C=1.568$ $\epsilon=4.63$ $r_e=0.9706$
H-O ($^4\Sigma$)	MP	$C=1.331$ $\epsilon=4.22$ $r_e=1.0121$
H-O ($^4\Pi$)		
H-O ($^4\Sigma$)		

The parameters are chosen so that $V(r)$ is in electron volts and r is in Angstroms.

Table 40

Transport Collision Integrals for the C-H Interaction

$T \times 10^{-3} \text{ (}^\circ\text{K)}$	$\sigma_{\Omega}^2(1,1)^* \text{ (}\text{\AA}^2\text{)}$	$\sigma_{\Omega}^2(2,2)^* \text{ (}\text{\AA}^2\text{)}$	A^*	B^*
1	8.9178	8.8958	1.0476	1.1807
2	7.3553	7.3080	1.0543	1.2066
3	6.4580	6.4967	1.0672	1.2354
4	5.8014	5.9626	1.0840	1.2659
5	5.2802	5.5599	1.1023	1.2915
6	4.8347	5.2158	1.1198	1.3106
7	4.4532	4.9091	1.1357	1.3229
8	4.1314	4.6392	1.1497	1.3297
9	3.8412	4.3851	1.1623	1.3324
10	3.5931	4.1566	1.1728	1.3319
11	3.3715	3.9455	1.1819	1.3299
12	3.1821	3.7564	1.1891	1.3251
13	3.0094	3.5790	1.1953	1.3232
14	2.8527	3.4136	1.2003	1.3199
15	2.7140	3.2625	1.2041	1.3169
16	2.5917	3.1257	1.2068	1.3145
17	2.4820	3.0001	1.2086	1.3132
18	2.3786	2.8795	1.2096	1.3129
19	2.2932	2.7779	1.2100	1.3137
20	2.2062	2.6722	1.2093	1.3160
21	2.1363	2.5866	1.2086	1.3188
22	2.0645	2.4969	1.2070	1.3238
23	2.0066	2.4234	1.2052	1.3290
24	1.9463	2.3454	1.2022	1.3372
25	1.8945	2.2778	1.1997	1.3454

Table 41

Transport Collision Integrals for the H-O Interaction

$T \times 10^{-3} \text{ (}^\circ\text{K)}$	$\sigma_{\Omega}^{2(1,1)*} \text{ (}\text{\AA}^2\text{)}$	$\sigma_{\Omega}^{2(2,2)*} \text{ (}\text{\AA}^2\text{)}$	A^*	B^*
1	12.7841	11.0176	0.8636	1.1570
2	10.7138	9.1133	0.8521	1.1792
3	9.5289	8.1146	0.8525	1.2178
4	8.6459	7.4967	0.8674	1.2738
5	7.9063	7.0463	0.8911	1.3310
6	7.2735	6.6820	0.9183	1.3792
7	6.7162	6.3587	0.9462	1.4163
8	6.1758	6.0315	0.9759	1.4449
9	5.7258	5.7419	1.0019	1.4616
10	5.3050	5.4542	1.0272	1.4716
11	4.9335	5.1825	1.0496	1.4744
12	4.5980	4.9231	1.0698	1.4735
13	4.2928	4.6725	1.0877	1.4690
14	3.9961	4.4153	1.1042	1.4620
15	3.7675	4.2061	1.1158	1.4551
16	3.5385	3.9886	1.1267	1.4475
17	3.3392	3.7904	1.1346	1.4406
18	3.1485	3.5929	1.1408	1.4346
19	2.9966	3.4295	1.1442	1.4307
20	2.8513	3.2681	1.1461	1.4283
21	2.7128	3.1091	1.1461	1.4281
22	2.5815	2.9582	1.1440	1.4304
23	2.4816	2.8309	1.1409	1.4347
24	2.3787	2.7001	1.1354	1.4432
25	2.2888	2.5835	1.1292	1.4535

Table 42

Interaction Potential Parameters for the C-O Interaction

<u>State</u>	<u>Potential</u>	<u>Parameters</u>
1_{Σ}^{+}	MP	$C=1.902 \quad \epsilon=11.242 \quad r_e=1.1281$
$1_{\Sigma_2}^{+}$		
3_{Σ}^{+}		
5_{Σ}^{+}		
$5_{\Sigma_2}^{+}$		
1_{Σ}^{-}		
3_{Σ}^{-}		
5_{Σ}^{-}		
1_{Π}		
1_{Π_2}		
3_{Π}		
3_{Π_2}		
5_{Π}		
5_{Π_2}		
1_{Δ}		
3_{Δ}		
5_{Δ}		
$3_{\Sigma_2}^{+}$		

The parameters are chosen so that $V(r)$ is in electron volts and r is in Angstroms.

Table 43

Transport Collision Integrals for the C-O Interaction

$T \times 10^{-3} \text{ (}^\circ\text{K)}$	$\sigma_{\Omega}^{2(1,1)*} (\text{\AA}^2)$	$\sigma_{\Omega}^{2(2,2)*} (\text{\AA}^2)$	A^*	B^*
1	14.6822	14.7130	1.0019	1.1922
2	12.8838	11.7392	0.9112	1.1183
3	11.8634	10.7609	0.9070	1.1579
4	11.1015	9.9934	0.9001	1.1711
5	10.5146	9.3813	0.8922	1.1742
6	10.0351	8.8927	0.8862	1.1779
7	9.6363	8.5095	0.8831	1.1851
8	9.2627	8.1775	0.8829	1.1970
9	8.9388	7.9137	0.8854	1.2121
10	8.6644	7.7073	0.8896	1.2283
11	8.3841	7.5108	0.8959	1.2477
12	8.1546	7.3590	0.9025	1.2654
13	7.9194	7.2101	0.9105	1.2846
14	7.6780	7.0621	0.9198	1.3052
15	7.4613	6.9318	0.9291	1.3239
16	7.2713	6.8183	0.9377	1.3402
17	7.0774	6.7023	0.9470	1.3565
18	6.8796	6.5831	0.9569	1.3726
19	6.7118	6.4805	0.9655	1.3857
20	6.5414	6.3747	0.9745	1.3983
21	6.3688	6.2652	0.9837	1.4103
22	6.1940	6.1518	0.9931	1.4216
23	6.0528	6.0581	1.0008	1.4299
24	5.8749	5.9372	1.0106	1.4395
25	5.7316	5.8372	1.0184	1.4463

Table 44

Mole Fractions of Species at the Surface of the Entry Probe
During Jovian Entry for Stagnation-Point Peak Heating

<u>Species</u>	<u>Mole Fraction</u>
C_3	0.303
H	0.149
C_4H	0.138
C_2H	0.115
CO	0.108
C_3H	0.099
C_2	0.028
C	0.026
H_2	0.024
C_2H_2	0.010
Total	1.000

Table 45

Transport Collision Integrals for the CO-CO Interaction

$T \times 10^{-3} \text{ (}^\circ\text{K)}$	$\sigma_{\Omega}^{2(1,1)*} \text{ (}\text{\AA}^2\text{)}$	$\sigma_{\Omega}^{2(2,2)*} \text{ (}\text{\AA}^2\text{)}$
1	7.9131	8.7386
2	7.1140	7.9304
3	6.6994	7.4950
4	6.4173	7.1974
5	6.2154	6.9724
6	6.0568	6.7999
7	5.9256	6.6571
8	5.8179	6.5386
9	5.7251	6.4348
10	5.6446	6.3461
11	5.5750	6.2703
12	5.5493	6.2429
13	5.5282	6.2214
14	5.5168	6.2136
15	5.5189	6.2141
16	5.5264	6.2262
17	5.5409	6.2458
18	5.5645	6.2720
19	5.5901	6.3033
20	5.6250	6.3442
21	5.6635	6.3889
22	5.7037	6.4404
23	5.7527	6.4933
24	5.8026	6.5522
25	5.8581	6.6167

Table 46

Interaction Potential Energy for the He-C₂H Interaction

r (Å)	V (He-C ¹) _{av}	V (He-C ²) _{av}	V (He-H ³) _{av}	V (He-C ₂ H) _{av}	V (ER)
1.85	3.18	0.30	0.59	4.07	3.88
1.90	2.32	0.25	0.44	3.01	3.01
1.95	1.73	0.22	33	2.28	2.33
2.00	1.31	0.19	0.25	1.75	1.81
2.05	1.01	0.16	0.20	1.36	1.40
2.10	0.78	0.14	0.15	1.07	1.09
2.15	0.62	0.12	0.12	0.86	0.84
2.18	0.54	0.11	0.11	0.75	0.72

Potential energy is in electron volts

Table 47

Transport Collision Integrals for the He-C₂H Interaction

$T \times 10^{-3} \text{ (}^\circ\text{K)}$	$\sigma_{\Omega}^{2(1,1)*} \text{ (}\text{\AA}^2\text{)}$	$\sigma_{\Omega}^{2(2,2)*} \text{ (}\text{\AA}^2\text{)}$
1	6.0301	6.8363
2	5.3911	6.1483
3	5.0422	5.7696
4	4.7966	5.5025
5	4.6144	5.3040
6	4.4599	5.1355
7	4.3399	5.0043
8	4.2371	4.8919
9	4.1433	4.7894
10	4.0584	4.6963
11	3.9895	4.6208
12	3.9212	4.5459
13	3.8610	4.4798
14	3.8087	4.4224
15	3.7568	4.3653
16	3.7053	4.3086
17	3.6614	4.2603
18	3.6250	4.2203
19	3.5832	4.1725
20	3.5455	4.1328
21	3.5097	4.0933
22	3.4812	4.0619
23	3.4458	4.0228
24	3.4175	3.9916
25	3.3894	3.9606

Table 48

The Binary Diffusion Coefficient, D (cm^2/sec), for the He- C_2H Interaction

$T \times 10^{-3}$ ($^{\circ}\text{K}$)	D (this report)	D (Esch, et al. ⁷²)
1	5.244	4.628
2	16.59	14.58
3	32.59	28.54
4	52.74	45.96
5	76.62	66.51
6	104.2	89.95
7	134.9	116.1
8	163.9	144.8
9	206.1	176.0
10	246.4	209.6
11	289.2	245.4
12	335.2	283.5
13	383.9	323.6
14	434.9	365.9
15	489.0	410.1
16	546.2	456.4
17	605.4	535.4
18	666.2	554.8
19	730.9	606.7
20	797.8	660.5
21	867.1	716.1
22	937.4	773.4
23	1012	832.5
24	1088	893.3
25	1166	955.8

Table 49
Interaction Potential Energy for the C-C₂ Interaction
for the $^1\Sigma_g^+$ State of C₂

r (Å)	V (C-C ₂) _{av}	V (Morse)
0.010	-874585	
0.200	-9174	
0.500	180.7	
0.550	231.5	
0.600	234.6	449.9
0.800	123.5	149.7
1.000	39.58	41.03
1.242	1.42	1.15
1.323	-3.10	-3.28
1.429	-6.02	-6.07
1.560	-6.93	-6.93
1.588	-6.90	-6.90
1.852	-5.17	-5.27
2.117	-3.14	-3.31
2.646	-0.96	-1.09
3.704	-0.07	-0.10
5.292	0	0
6.000	0	0

Potential energy is in electron volts

Table 50
Transport Collision Integrals for the C-C₂ Interaction

$T \times 10^{-3} \text{ (}^\circ\text{K)}$	for the $^1\Sigma_g^+$ State of C ₂			
	$\sigma_{\Omega}^{2(1,1)*} (\text{\AA}^2)$	$\sigma_{\Omega}^{2(2,2)*} (\text{\AA}^2)$	A*	B*
1	13.9192	13.2872	0.9546	1.1074
2	12.1639	11.3227	0.9308	1.1541
3	11.1142	10.2096	0.9186	1.1660
4	10.3457	9.4087	0.9094	1.1715
5	9.7603	8.8495	0.9067	1.1846
6	9.2741	8.4349	0.9095	1.2051
7	8.8299	8.0963	0.9169	1.2317
8	8.4562	7.8359	0.9267	1.2587
9	8.0981	7.6006	0.9386	1.2871
10	7.7569	7.3835	0.9519	1.3151
11	7.4680	7.2009	0.9642	1.3386
12	7.1701	7.0108	0.9778	1.3617
13	6.8982	6.8335	0.9906	1.3813
14	6.6551	6.6705	1.0023	1.3974
15	6.4077	6.4996	1.0143	1.4119
16	6.1568	6.3201	1.0265	1.4246
17	5.9395	6.1593	1.0370	1.4339
18	5.7574	6.0204	1.0456	1.4402
19	5.5380	5.8481	1.0559	1.4462
20	5.3551	5.6999	1.0644	1.4497
21	5.1725	5.5480	1.0726	1.4517
22	5.0269	5.4240	1.0790	1.4520
23	4.8459	5.2663	1.0867	1.4520
24	4.7023	5.1382	1.0927	1.4506
25	4.5598	5.0038	1.0984	1.4484

Table 51
Interaction Potential Energy for the C_2-C_2 Interaction
for the $1\Sigma_g^+$ State of C_2

r (Å)	$V(C_2-C_2)_{av}$	$V(\text{Morse})$
0.100	-732400	
0.300	-65574	
0.600	-3393	
0.900	10.05	
1.000	81.04	
1.058	83.55	188.3
1.323	27.97	34.99
1.429	11.41	13.19
1.588	-2.21	-2.16
1.852	-7.92	-7.91
1.867	-7.92	-7.92
2.117	-6.41	-6.49
2.646	-2.34	-2.58
3.704	-0.19	-0.27
4.000	-0.09	-0.14
4.292	0	-0.07
5.000	0.01	-0.02
6.000	0	0

Potential energy is in electron volts

Table 52

Transport Collision Integrals for the C_2-C_2 Interaction for

$T \times 10^{-3}$ ($^{\circ}K$)	the $^1\Sigma_g^+$ State of C_2	
	$\sigma_{\Omega}^{2(1,1)*}$ (\AA^2)	$\sigma_{\Omega}^{2(2,2)*}$ (\AA^2)
1	18.6803	20.5068
2	16.4601	17.0317
3	15.2878	15.5781
4	14.4943	14.7858
5	13.8734	14.1219
6	13.3545	13.5339
7	12.8881	13.0009
8	12.5060	12.5760
9	12.1494	12.1983
10	11.8476	11.8963
11	11.5397	11.6059
12	11.2875	11.3806
13	11.0290	11.1597
14	10.7630	10.9413
15	10.5234	10.7502
16	10.3126	10.5851
17	10.0966	10.4176
18	9.8753	10.2466
19	9.6867	10.1008
20	9.4945	9.9513
21	9.2988	9.7977
22	9.0997	9.6397
23	8.9382	9.5098
24	8.7338	9.3431
25	8.5684	9.2060

Table 53

Comparison of the C-C, C-C₂, and C₂-C₂ InteractionPotentials Corresponding to the $^1\Sigma_g^+$ State of C₂

$r(\text{\AA})$	$V(\text{C-C})$	$V(\text{C-C}_2)$	$V(\text{C}_2\text{-C}_2)$
1.058	-4.42	25.68	83.55
1.111	-5.49	16.05	75.75
1.242	-6.36	1.42	45.01
1.323	-6.15	-3.10	27.97
1.429	-5.47	-6.02	11.41
1.588	-4.15	-6.90	-2.21
1.852	-2.26	-5.17	-7.92
2.117	-1.13	-3.14	-6.41
2.646	-0.29	-0.96	-2.34
3.704	-0.03	-0.07	-0.19
5.292	0	0	0

Potential energy is in electron volts

Table 54

The Translational Contribution to the Thermal Conductivity, λ_{tr}^{mix} (W/m/°K),
for a Mixture of C and C₂

<u>$T \times 10^{-3} (^{\circ}K)$</u>	<u>$X=0.00$</u>	<u>$X=0.25$</u>	<u>$X=0.50$</u>	<u>$X=0.75$</u>	<u>$X=1.00$</u>
4	0.03	0.117	0.134	0.157	0.195
5	0.120	0.139	0.159	0.187	0.231
6	0.137	0.159	0.184	0.216	0.267
7	0.155	0.180	0.207	0.244	0.301
8	0.177	0.199	0.230	0.271	0.334

The symbol X denotes the mole fraction of carbon atoms.

Table 55

Transport Collision Integrals for the He-0 Interaction

$T \times 10^{-3} \text{ (}^\circ\text{K)}$	$\sigma_{\Omega}^{2(1,1)*} (\text{\AA}^2)$	$\sigma_{\Omega}^{2(2,2)*} (\text{\AA}^2)$	A^*	B^*
1	2.3220	2.7032	1.1654	1.1279
2	2.0096	2.3584	1.1748	1.1368
3	1.8348	2.1645	1.1809	1.1427
4	1.7162	2.0322	1.1854	1.1471
5	1.6288	1.9346	1.1890	1.1507
6	1.5590	1.8564	1.1921	1.1538
7	1.4982	1.7883	1.1948	1.1566
8	1.4498	1.7339	1.1972	1.1589
9	1.4058	1.6843	1.1994	1.1612
10	1.3696	1.6436	1.2013	1.1631
11	1.3340	1.6034	1.2032	1.1651
12	1.3023	1.5675	1.2049	1.1669
13	1.2745	1.5360	1.2065	1.1686
14	1.2504	1.5087	1.2079	1.1700
15	1.2265	1.4817	1.2093	1.1715
16	1.2062	1.4586	1.2106	1.1728
17	1.1861	1.4358	1.2118	1.1741
18	1.1662	1.4131	1.2130	1.1754
19	1.1476	1.3907	1.2143	1.1768
20	1.1301	1.3720	1.2154	1.1780
21	1.1138	1.3536	1.2165	1.1791
22	1.1010	1.3389	1.2174	1.1801
23	1.0850	1.3206	1.2184	1.1812
24	1.0723	1.3061	1.2193	1.1822
25	1.0596	1.2916	1.2202	1.1832

Table 56
Transport Collision Integrals for the He-C Interaction

$T \times 10^{-3} \text{ (}^\circ\text{K)}$	$\sigma_{\Omega}^2(1,1)^* \text{ (}\text{\AA}^2\text{)}$	$\sigma_{\Omega}^2(2,2)^* \text{ (}\text{\AA}^2\text{)}$
1	4.2921	5.2846
2	3.4359	4.2304
3	3.0166	3.7141
4	2.7505	3.3865
5	2.5604	3.1524
6	2.4148	2.9732
7	2.2982	2.8297
8	2.2018	2.7110
9	2.1201	2.6104
10	2.0496	2.5236
11	1.9879	2.4475
12	1.9331	2.3801
13	1.8841	2.3197
14	1.8398	2.2652
15	1.7995	2.2156
16	1.7626	2.1702
17	1.7286	2.1283
18	1.6972	2.0896
19	1.6680	2.0537
20	1.6407	2.0202
21	1.6152	1.9888
22	1.5913	1.9593
23	1.5688	1.9315
24	1.5475	1.9053
25	1.5273	1.8805

$$A^* = 1.2312$$

$$B^* = 1.1792$$

Table 57

Transport Collision Integrals for the C^+-H Interaction

$T \times 10^{-3} \text{ (}^\circ\text{K)}$	$\sigma_{\Omega}^2(1,1)^* \text{ (}\text{\AA}^2\text{)}$	$\sigma_{\Omega}^2(2,2)^* \text{ (}\text{\AA}^2\text{)}$	A^*	B^*
1	11.0850	10.2919	0.9675	1.1640
2	9.0892	8.4479	0.9759	1.2266
3	7.9100	7.5014	1.0004	1.2822
4	6.9759	6.8435	1.0295	1.3278
5	6.2486	6.3261	1.0571	1.3585
6	5.6166	5.8630	1.0832	1.3776
7	5.0940	5.4561	1.1052	1.3860
8	4.6573	5.0982	1.1238	1.3881
9	4.2643	4.7581	1.1401	1.3854
10	3.9273	4.4508	1.1535	1.3804
11	3.6442	4.1795	1.1639	1.3748
12	3.3872	3.9230	1.1722	1.3688
13	3.1676	3.6944	1.1783	1.3639
14	2.9826	3.4945	1.1821	1.3606
15	2.8099	3.3024	1.1844	1.3586
16	2.6554	3.1244	1.1840	1.3587
17	2.5238	2.9688	1.1838	1.3609
18	2.4124	2.8341	1.1820	1.3648
19	2.2977	2.6813	1.1781	1.3720
20	2.2033	2.5707	1.1738	1.3813
21	2.1191	2.4604	1.1680	1.3932
22	2.0511	2.3696	1.1626	1.4059
23	1.9742	2.2639	1.1546	1.4250
24	1.9163	2.1824	1.1473	1.4440
25	1.8616	2.1038	1.1391	1.4666

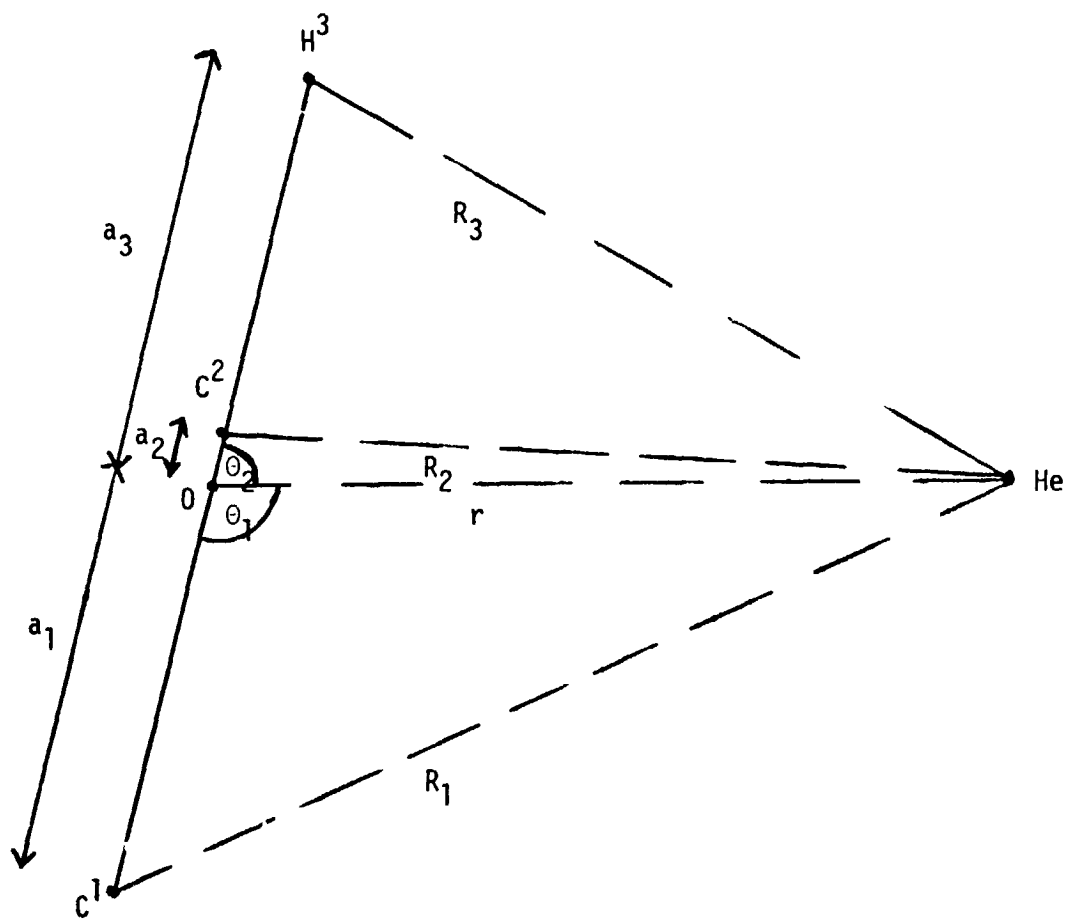
Table 58

Transport Collision Integrals for the C-C⁺ Interaction

$T \times 10^{-3} \text{ (}^\circ\text{K)}$	$\sigma_{\Omega}^{2,2} (2,2)^* \text{ (}\text{\AA}^2\text{)}$	A^*	B^*
1	6.9224	1.1257	1.1017
2	6.1607	1.1118	1.1012
3	5.7784	1.1049	1.1178
4	5.4646	1.0971	1.1199
5	5.2200	1.0896	1.1182
6	5.0279	1.0851	1.1214
7	4.8674	1.0824	1.1310
8	4.7462	1.0817	1.1433
9	4.6358	1.0828	1.1570
10	4.5398	1.0840	1.1709
11	4.4492	1.0861	1.1849
12	4.3667	1.0888	1.1976
13	4.2884	1.0914	1.2091
14	4.2142	1.0942	1.2193
15	4.1408	1.0971	1.2282
16	4.0728	1.0998	1.2356
17	4.0030	1.1024	1.2423
18	3.9364	1.1050	1.2476
19	3.8705	1.1074	1.2519
20	3.8076	1.1095	1.2552
21	3.7458	1.1114	1.2574
22	3.6875	1.1131	1.2588
23	3.6268	1.1146	1.2598
24	3.5706	1.1160	1.2598
25	3.5161	1.1172	1.2599

Figure 1

Coordinate System for the He-C₂H Interaction



0 = center of geometry

$$a_1 = a_3 = 1.134 \text{ \AA} \quad a_2 = 0.073 \text{ \AA}$$

$$\theta_2 = \theta_3$$

Publications

- L. Biolsi
"Transport Properties in the Jovian Atmosphere"
Journal of Geophysical Research, 83, 1125 (1978).
- L. Biolsi
"Transport Properties of Monatomic Carbon"
Journal of Geophysical Research, 83, 2476 (1978).
- L. Biolsi and L. R. Wallace
"Some Effects of Ablation on Transport Properties in the Jovian Atmosphere"
Progress in Astronautics and Aeronautics: Thermal Protection Systems
(in press).

Presentations

- L. Biolsi
"Effect of Surface Ablation on Transport Properties in a H_2 -He Atmosphere"
173rd National Meeting, American Chemical Society
New Orleans, LA, March 20-25, 1977.
- L. Biolsi
"Transport Properties in the Atmosphere of Jupiter"
13th Midwest Regional Meeting, American Chemical Society
Rolla, MO, Nov. 3-4, 1977.
- L. Biolsi
"Transport Properties of Gaseous Carbon"
33rd Southwest Regional Meeting, American Chemical Society
Little Rock, AR, Dec. 5-7, 1977.
- L. Biolsi
"Some Effects of Ablation on Transport Properties in the Jovian Atmosphere"
2nd AIAA/ASME Thermophysics and Heat Transfer Conference
Palo Alto, CA, May 24-26, 1978.
- L. Biolsi and K. J. Biolsi
"The Thermal Conductivity of Carbon in Electronically Excited States"
14th Midwest Regional Meeting, American Chemical Society
Fayetteville, AR, Oct. 26-27, 1978.
- L. Biolsi and L. R. Wallace
"Transport Properties in a C_2 -C System"
14th Midwest Regional Meeting, American Chemical Society
Fayetteville, AR, Oct. 26-27, 1978.